Electronic Supporting Information for the article

Phosphorescent O_2-probes Based on Ir(III) Complexes for Bioimaging Applications

Mozhgan Samandarsangari [1], Ilya S. Kritchenkov [1], Daria O. Kozina [1], Anastasia D. Komarova [2,3], Marina V. Shirmanova [2], Sergey P. Tunik [1]*

[1]St. Petersburg State University, Universitetskaya Embankment 7-9, 199034 St. Petersburg, Russia

[2]Privolzhskiy Research Medical University, Institute of Experimental Oncology and Biomedical Technologies, Minin and Pozharsky sq. 10/1, 603005 Nizhny Novgorod, Russia

[3]Lobachevsky State University of Nizhny Novgorod, Gagarina av., 23, 603950, Nizhny Novgorod, Russia

Synthesis of Ligands and Complexes

Synthesis of N^C ligand. The following components were placed in a 5 mL vial: 4-(2-pyridyl)benzoic acid (200.0 mg, 1.004 mmol), NH_2-2OEG (354.4 mg, 1.200 mmol), N,N′ dicyclohexylcarbodiimide (247.6 mg, 1.200 mmol), N-hydroxysuccinimide (138.1 mg, 1.200 mmol), 4-(dimethylamino) pyridine (3.6 mg, 0.03 mmol), triethylamine (121.4 mg, 1.200 mmol) and dry DMSO (1.0 mL). The reaction mixture was stirred for 4 days at RT and thoroughly evaporated. The dried residue was suspended in 3 mL of water and cooled. Then the solution was isolated by centrifugation and vacuum-dried to give the oily substance. It was dissolved in DCM cooled for 1 day, centrifuged and thoroughly dried. The dried residue was dissolved in 100 mL of chloroform and sequentially washed with 20 mL of brine (with 0.2 g of citric acid monohydrate), and with 20 mL of pure brine. The organic layer was dried over Na_2SO_4, then filtered and evaporated to give the oily substance. It was dissolved in EtOAc/n-hexane 5:1 mixture, and purified using column chromatography (sequentially eluted with EtOAc and EtOAc/methanol 5:1 mixture). After evaporation of combined fractions, the resulting ligand was obtained as colorless viscous oil. 208 mg, yield 44%. ^{1}H NMR ($CDCl_3$, 400 MHz, δ): 8.74 (d, J = 4.7 Hz, 1H), 8.08 (d,

J = 8.3 Hz, 2H), 7.94 (d, J = 8.3 Hz, 2H), 7.83-7.78 (m, 2H), 7.33-7.29 (m, 1H), 6.88 (d, J = 8.1 Hz, 1H, NH), 4.48 (m, 1H, CH), 3.81-3.66 (m, 20H, CH_2), 3.55 (m, 6H, CH_3). HRMS (ESI) m/z: 477.2580 calculated for $C_{25}H_{37}N_2O_7^+$ $[M + H]^+$, found 477.2601

Synthesis of N^N1 ligand. 4,4′-bipyridine-dicarboxylic acid (200.0 mg, 0.819 mmol), NH_2-2OEG (580.7 mg, 1.966 mmol), N,N′ dicyclohexylcarbodiimide (405.3 mg, 1.966 mmol), N-hydroxysuccinimide (226.3 mg, 1.966 mmol), 4-(dimethylamino) pyridine (6.0 mg, 0.049 mmol), triethylamine (199.0 mg, 1.966 mmol) and dry DMSO (2.0 mL) were put in 5 ml vial and closed with a cap. The reaction mixture was stirred for 4 days at 45 °C then 1 drop of water was added to quench the DCC and stirred for 12 h and thoroughly evaporated. The dried residue was suspended in 3 mL of water and cooled for 2 days. Then the solution was isolated by centrifugation and vacuum-dried to give the oily substance. It was dissolved in DCM, cooled for 1 day, centrifuged and was thoroughly dried. The residue was dissolved in 10 mL diethyl ether, heated into boiling point for 5 minutes and cooled for 1 day to do recrystallization. The solvent was decanted and the precipitate was vacuum dried and dissolved in DCM (0.6 mL), diluted with n-hexane (5 mL), and heated in 65 °C for 10 minutes, the solvent was decanted, and the oily residue was thoroughly vacuum-dried. The dried residue was dissolved in 80 mL of chloroform and sequentially washed with 20 mL of 1:1 brine/water (with addition of 0.3 g of citric acid monohydrate), 20 mL of 1:1 brine/water (with addition of 0.3 g of potassium carbonate), 20 mL of pure 1:1 brine/water and with 10 mL of pure brine. The organic layer was dried over Na_2SO_4, then filtered and evaporated to give the oily substance. It was dissolved in MeCN, cooled for 1 day, centrifuged and the solution was thoroughly dried. The substance was dissolved in chloroform and purified using column chromatography (sequentially eluted with chloroform and chloroform/methanol 20:1, 10:1 mixture). The collected fractions were combined and vacuum dried to give the desired product. 110 mg, Yield 17%. ^{1}H NMR ($(CD_3)_2CO$, 400 MHz, δ): 8.86 (s, 1H), 8.83 (d, J = 5.0 Hz, 1H), 7.99 (d, J = 8.0 Hz, 1H, NH) 7.85 (dd, J = 5.0 Hz, J = 1.7 Hz, 1H), 4.45 (m, 1H, CH), 3.76-3.29 (m, 20H, CH_2), 3.25 (m, 6H, CH_3). HRMS (ESI) m/z: 799.4263 calculated for $C_{38}H_{63}N_4O_{14}^+$ $[M + H]^+$, found 799.4341

Synthesis of 4-Oxo-4-((1-(pyridin-2-yl)-1H-1,2,3-triazol-4-yl)methoxy)-butanoic acid. In a 50 mL round-bottom flask were placed 2-azidopyridine (312.0 mg, 2.60 mmol), 4-oxo-4-(prop-2-yn-1-yloxy)butanoic acid (405.6 mg, 2.60 mmol), $CuSO_4 \cdot 5H_2O$ (649.2 mg, 2.60 mmol), sodium ascorbate (1030.2 mg, 5.20 mmol), DMF (25 mL). The flask was closed with a septum, and the

reaction mixture was stirred for 7 days at 60 °C in the absence of light. Then the resulting suspension was placed in a separating funnel, diluted with chloroform (200 mL), and thoroughly washed three times with a water/brine mixture (1:1, 50 mL). The organic layer was dried over anhydrous Na_2SO_4, filtered, and evaporated. The residue was dissolved in chloroform (3 mL), diluted with n-heptane (20 mL), and evaporated to a volume of ca. 10 mL. The solvent was decanted, and the oily residue was thoroughly vacuum-dried and put in a freezer for several hours. Further purifying of the oily substance was done by washing with 8 mL of water (2 × 4 mL), centrifuged and the precipitate was evaporated to dryness. 343 mg, yield 48%. ^{1}H NMR ($(CD_3)_2CO$, 400 MHz, δ): 8.73 (s, 1H), 8.58 (d, J = 4.0 Hz, 1H), 8.19 (d, J = 8.0 Hz, 1H), 8.73 (s, 1H), 8.58 (d, J = 5.0 Hz, 1H), 8.18 (d, J = 8.1 Hz, 1H), 8.12 (dd, J = 7.3 Hz, J = 8.1 Hz, 1H), 7.53 (dd, J = 5.0 Hz, 7.3 Hz, 1H), 5.31 (s, 2H, CH_2), 2.65 (m, 4H, CH_2CH_2).

Synthesis of N^N2 ligand. The following components were placed in a 5 mL vial: 4-Oxo-4-((1-(pyridin-2-yl)-1H-1,2,3-triazol-4-yl)methoxy)-butanoic Acid (140.0 mg, 0.51 mmol), NH_2-2OEG (177.2 mg, 0.60 mmol), N,N′ dicyclohexylcarbodiimide (123.8 mg, 0.60 mmol), N-hydroxysuccinimide (69.1 mg, 0.60 mmol), 4-(dimethylamino) pyridine (2.2 mg, 0.018 mmol), triethylamine (60.7 mg, 0.60 mmol) and dry DMSO (1.0 mL). The reaction mixture was stirred for 4 days at RT then 1 drop of water was added to quench the DCC and stirred for 48 h, then reaction mixture was thoroughly evaporated. The dried residue was suspended in 6 mL of water and centrifuged, the aqueous solution cooled for 1 day, then was centrifuged again and vacuum-dried. The oily residue was dissolved in DCM, cooled for 1 day, centrifuged and the solution was thoroughly dried. The oily residue was precipitated with adding Et_2O (3 mL), solution was decanted and the residue was thoroughly dried. The oily residue was washed by using 4 mL of n-heptane, the n-heptane solution was decanted and the residue was vacuum dried. The obtained oily residue was dissolved in EtOAc, and purified using column chromatography (sequentially eluted with EtOAc and EtOAc/methanol 20:1, 10:1 mixture). After evaporation of collected fractions, the resulting ligand was obtained as colorless viscous oil. 137 mg, yield 49%. ^{1}H NMR ($(CD_3)_2CO$, 400 MHz, δ): 8.75 (s, 1H), 8.59 (d, J = 5.0 Hz, 1H), 8.18 (d, J = 8.3 Hz, 1H), 8.12 (dd, J = 8.3 Hz, J = 7.4 Hz, 1H), 7.53 (dd, J = 7.4 Hz, J = 5.0 Hz, 1H), 6.98 (d, J = 8.0 Hz, 1H, NH), 5.29 (s, 2H, CH_2), 4.12 (m, 1H, CH), 3.59–3.45 (m, 20H, CH_2), 3.29 (s, 6H, CH_3), 2.64 (t, J = 7.0 Hz, 2H), 2.52 (t, J = 7.0 Hz, 2H).

Synthesis of 4-(2-(pyridin-2-yl)-1H-phenanthro [9,10-d]imidazol-1-yl)benzoic acid. Phenanthrene-9,10-dione (2.0 g, 9.330 mmol), 4-aminobenzoic acid (3.2 g, 23.325 mmol), picolinaldehyde (1.0 g, 9.330 mmol), ammonium acetate (1.8 g, 23.325 mmol), and 30 mL of glacial acetic acid were stirred at 70 °C in a 100 mL round-bottom flask. After 3 h, the solution was evaporated. The resulted oil was dissolved in 0.5 mL of acetone and 0.5 mL of dichloromethane then 10 mL of water was added and it turned to a beige precipitate. It was centrifuged and the precipitate was washed with diethyl ether and dissolved in 2 ml of DMSO and left for 24 h. The black precipitate was formed and the suspension was centrifuged. Then 10 mL of water was added to the obtained solution and the white precipitate was formed. This solid was centrifuged and finally dried under vacuum. 390 mg, yield 10%. ^{1}H NMR ($(CD_3)_2SO$, 400 MHz, δ): 13.26 (br s, 1H), 8.94 (d, J = 8.4 Hz, 1H), 8.89 (d, J = 8.4 Hz, 1H), 8.72 (d, J = 7.8, 1H), 8.28 (d, J = 7.3 Hz, 2H), 8.16 (d, J = 8.4 Hz, 2H), 7.94 (t, J = 8.0 Hz, 1H), 7.82-7.69 (m, 4H), 7.58 (t, J = 7.9, 1H), 7.39-7.32 (m, 2H), 7.04 (d, J = 8.4, 1H).

Synthesis of N^N3 ligand. 4-(2-(pyridin-2-yl)-1H-phenanthro [9,10-d]imidazol-1-yl)benzoic acid (207.7 mg, 0.50 mmol), the corresponding amine NH_2-2OEG (177.2 mg, 0.6 mmol), N,N′ dicyclohexylcarbodiimide (123.8 mg, 0.60 mmol), N-hydroxysuccinimide (69.1 mg, 0.60 mmol), 4-(dimethylamino) pyridine (1.8 mg, 0.015 mmol), triethylamine (60.7 mg, 0.60 mmol) and dry DMSO (1 mL) were placed in a 5 mL vial. The reaction mixture was stirred for 5 days at RT and then 1 drop of water was added to quench the DCC, stirred for 24 h, and thoroughly evaporated. The dried residue was suspended in 3 mL of ethylacetate/toluene and cooled for 2 days. Then the solution was isolated by centrifugation and vacuum-dried to give the oily substance. It was dissolved in DCM, cooled for 3 days, centrifuged and was thoroughly dried. The oily residue was washed using diethyl ether and n-heptane respectively for 3 times using ultrasound bath. After decantation and evaporation, the residue was dissolved in 0.2 mL DCM then 4 mL n-heptane was added, decanted and the oily residue was dried. Further purifying of the oily substance was done dissolving in EtOAc, and using column chromatography (sequentially eluted with EtOAc/hexane 5:1 mixture, EtOAc and EtOAc/methanol 10:1 mixture). The collected fractions were combined and vacuum dried. 162 mg, yield 47%.^{1}H NMR ($(CD_3)_2CO$, 400 MHz, δ): 8.95 (d, J = 8.3 Hz, 1H), 8.89 (d, J = 8.4 Hz, 1H), 8.85 (d, J = 8.0 Hz, 1H), 8.43 (d, J = 8.0 Hz, 1H), 8.31 (d, J = 4.8 Hz, 1H, NH), 8.19 (d, J = 8.4 Hz, 2H), 7.96 (dt, J = 7.8 Hz, J = 1.7 Hz, 1H), 7.84-7.72 (m, 5H), 7.61 (dt, J

= 7.8 Hz, J = 1.0 Hz 1H), 7.37-7.32 (m, 2H), 7.22 (d, J = 8.4 Hz, 1H), 4.51 (m, 1H, CH), 3.84-3.51 (m, 20H, CH_2), 3.30 (s, 6H, CH_3).

Synthesis of iridium dimeric complex [Ir_2(N^C_2)$_4$$Cl_2$]. $IrCl_3.6H_2O$ (105.0 mg, 0.26 mmol), the corresponding modified cyclometallating ligand (N^C, 246.0 mg, 0.51 mmol), 2-methoxyethanol (2.5 mL), and distilled water (10 mL) were placed in a 25 mL tall test tube and degassed for about 30 minutes. The reaction mixture was stirred at 100 °C for 48 hours. The resulting red solution was dried. The solid residue was washed with heptane, evaporated, dissolved in 1.5 mL of water, and centrifuged. The resulting solution was dried, dissolved in 1.5 mL of dichloromethane, centrifuged, and vacuum-dried. To remove impurities the dried residue was dissolved in 0.5 mL of chloroform and then precipitated by adding 15 mL of 3:1 Et_2O/heptane mixture. The solution was decanted and the oily residue was evaporated. This step was repeated two times. Then this oily residue was extracted (4 times × 10 mL) with ethylacetate and centrifuged. Then this solution was evaporated to dryness. 200 mg; Yield 33%. ^{1}H NMR ($(CD_3)_2SO$, 400 MHz, δ): 9.85 (d, J = 6.0 Hz, 1H), 9.56 (d, J = 5.8 Hz, 1H), 8.36 (d, J = 8.2 Hz, 1H) 8.28 (d, J = 7.9 Hz, 1H), 8.16 (t, J = 7.7, 1H), 8.07 t, J = 8.2, 1H), 7.90-7.83 (m, 2H), 7.80 (d, J = 8.1 Hz, 1H), 7.74 (d, J = 8.1 Hz, 1H), 7.63 (t, J = 6.6, 1H), 7.52 (t, J = 6.8, 1H), 7.34 (d, J = 8.1 Hz, 1H), 7.30 (d, J = 8.1 Hz, 1H), 6.73 (s, 1H), 6.16 (s, 1H), 4.05 (m, 1H, CH), 3.52-3.34 (m, 40H). 3.22 (s, 3H, CH_3), 3.21 (s, 3H, CH_3), 3.19 (s, 3H, CH_3), 3.18 (s, 3H, CH_3). HRMS (ESI) m/z: 1143.4729 calculated for $C_{50}H_{70}IrN_4O_{14}^+$ [Ir(N^C)$_2$]$^+$, found 1143.4520.

General procedure for the synthesis of iridium [Ir(N^C)$_2$(N^N#)]Cl complexes (Ir1–Ir3). The following components were placed in a 5 mL vial: the corresponding iridium dimeric complex (23.6 mg, 0.010 mmol), N^N# ligand (0.022 mmol) and methanol (1 mL). The reaction mixture was stirred for 24 h at RT and then they were worked up as follows.

Complex Ir1. The reaction mixture was evaporated, the obtained solid was dissolved in 0.2 mL of acetone and then precipitated by adding of 2.0 mL of Et_2O. Solution was decanted and the residue was thoroughly dried. The residue was dissolved in 0.7 mL of water, centrifuged, and the aqueous solution was vacuum dried. The dried residue was dissolved in 1 mL of Et_2O/EtOAC 1:1 mixture, centrifuged, and the obtained solution was vacuum dried. The residue was dissolved in 0.6 mL of water, centrifuged, and the solution was dried. The obtained solid was dissolved in 0.2 mL of chloroform and precipitated with mixture of 2.0 mL of Et_2O and 1.0 mL of n-hexane, the precipitate was separated by decanting the solution and vacuum-dried. Additional purification was

done by dissolving in chloroform followed by column chromatography (sequentially eluted with chloroform and chloroform/methanol 20:1, 10:1 mixture). The collected fractions were combined and vacuum dried. The residue was dissolved in 1.0 mL of water and centrifuged. Then the aqueous solution was evaporated to dryness. Furthermore, the residue was dissolved in acetone, centrifuged and the solution was finally vacuum-dried to give the desired product. 12 mg; Yield 30%. ^{1}H NMR (CD_3OD, 400 MHz, δ): 9.20 (s, 1H), 8.26 (d, J = 8.2 Hz, 1H), 8.15 (d, J = 5.6 Hz, 1H), 7.97-7.93 (m, 3H), 7.74 (d, J = 5.6 Hz, 1H), 7.47 (d, J = 8.3 Hz, 1H), 7.17 (t, J = 6.6 Hz, 1H), 6.75 (s, 1H), 4.44 (m, 1H, CH), 4.24 (m, 1H, CH), 3.74-3.41 (m, 40H, CH_2), 3.30 (s, 3H, CH_3), 3.25 (s, 3H, CH_3), 3.24 (s, 3H, CH_3), 3.23 (s, 3H, CH_3). HRMS (ESI) m/z: 982.4337 calculated for $C_{88}H_{132}IrN_8O_{28}^{2+}$ $[M + Na]^{2+}$, found 982.4533.

Complex Ir2. The reaction mixture was evaporated, the obtained solid was dissolved in 0.2 mL of acetone and precipitated with mixture of 2.0 mL of Et_2O and 1.0 mL of n-hexane, after decanting the precipitate was thoroughly dried. This step was repeated two times. The dried residue was dissolved in EtOAc, centrifuged, and the obtained solution was vacuum dried then was dissolved in 0.3 mL of water, centrifuged, and the aqueous solution was dried completely. The obtained solid was dissolved in 0.2 mL of acetone and then precipitated by adding of 2.0 mL of Et_2O. The precipitate was isolated and vacuum dried. The obtained residue was dissolved in chloroform and purified using column chromatography (sequentially eluted with chloroform and chloroform/methanol 20:1, 10:1 mixture). The collected fractions were combined and vacuum dried. The residue was dissolved in 1.0 mL of water and centrifuged. Then the water solution was evaporated to dryness then was dissolved in acetone, centrifuged and finally vacuum-dried to give the desired product. 16 mg; Yield 48%. ^{1}H NMR (CD_3OD, 400 MHz, δ): 9.45 (s, 1H), 8.54 (d, J = 8.3 Hz, 1H), 8.39 (t, Hz, J = 7.9, 1H), 8.25 (d, J = 7.9 Hz, 2H), 7.99 (t, Hz, J = 7.9, 2H), 7.95 (d, J = 7.8 Hz, 2H), 7.88 (d, J = 8.2 Hz, 1H), 7.84 (t, J = 6.8, 2H), 7.63 (t, J = 6.4 Hz, 1H), 7.47 (d, J = 8.3 Hz, 1H), 7.41 (d, J = 8.1 Hz, 1H), 7.23 (m, 2H), 6.73 (s, 1H), 6.70 (s, 1H), 5.27 (s, 2H, CH_2), 4.24 (m, 2H, CH), 4.06 (m, 1H, CH), 3.64-3.40 (m, 60 H), 3.33 (s, 6H, CH_3), 3.31 (s, 3H, CH_3), 3.30 (s, 3H, CH_3), 3.27 (s, 3H, CH_3), 3.26 (s, 3H, CH_3). HRMS (ESI) m/z: 859.8579 calculated for $C_{75}H_{109}IrN_9NaO_{23}^{2+}$ $[M + Na]^{2+}$, found 859.8640.

Complex Ir3. This complex was thoroughly vacuum dried. Then it was dissolved in 0.2 mL acetone and precipitated by adding 2.0 mL of Et_2O, decanted and the precipitate was vacuum dried, these sequences were repeated three times. Then it was dissolved in ethyl acetate, centrifuged, and

obtained solution was dried. The dried residue was washed three times with 6 mL of 2:1 EtOAc/E_2O mixture, centrifuged and the precipitate was vacuum dried. Further, the dried residue was dissolved in 1.0 mL of water, centrifuged and vacuum dried then was dissolved in acetone, centrifuged and finally vacuum-dried to give the desired product. 15 mg; Yield 40%. ^{1}H NMR (CD_3OD, 400 MHz, δ): 8.75 (d, 2H), 8.60 (d, J = 8.4 Hz, 1H), 8.48 (d, J = 8.0 Hz, 1H) 8.41-8.37 (m, 3H), 8.12 (d, J = 8.3, 1H), 8.05 (d, J = 7.9 Hz, 1H), 8.02 (d, J = 8.0 Hz, 1H), 7.95 (d, J = 5.2 Hz, 1H), 7.91 (d, J = 8.0 Hz, 1H), 7.86-7.82 (m, 2H), 7.80-7.77 (m, 2H), 7.61 (dd, J = 9.3 Hz, J = 8.1 Hz, 2H), 7.48 (d, J = 8.1 Hz, 1H), 7.44 (t, J = 7.8 Hz, 1H), 7.38 (t, J = 6.6 Hz, 1H), 7.33 (d, J = 8.2 Hz, 1H),7.31-7.23 (m, 3H), 7.08 (dd, J = 9.7, J = 9.3, 2H), 6.98 (s, 1H), 6.89 (t, J = 7.7, 1H), 6.66 (s, 1H), 4.53 (m, CH, 1H), 4.33 (m, CH, 1H), 4.21 (m, CH, 1H), 3.82-3.41 (m, 60H, CH_2), 3.33 (s, 6H, CH_3), 3.29 (s, 6H, CH_3), 3.27 (s, 3H, CH_3), 3.26 (s, 3H, CH_3). 929.3868 calculated for $C_{90}H_{114}IrN_8NaO_{21}^{2+}$ $[M + Na]^{2+}$, found 929.3811.

Experimental details

Photophysical experiments. Photophysical measurements were performed in aqueous media. Absorption spectra were recorded using Shimadzu UV-1800 spectrophotometer. The emission spectra were measured on Avantes AvaSpec-2048x64 spectrometer. The values of the absolute emission quantum yield in solution were measured using a comparative method, 365 nm LED as excitation source and $[Ru(bpy)_3][PF_6]_2$ water solution (Φ = 0.040 air-saturated, 0.063 Ar-saturated) as the reference. For the lifetime measurements pulse laser DTL-375QT (wavelength 355 nm, pulse width 5 ns, repetition frequency 1000 Hz), Hamamatsu (H10682-01) photon counting head, FASTComTec (MCS6A1T4) multiple-event time digitizer and Ocean Optics monochromator (Monoscan-2000, interval of wavelengths 1 nm) were used. PyroScience FireStingO2 oxygen meter, equipped with an oxygen sensor OXROB10 and a temperature sensor TDIP15, was used to measure concentration and partial pressure of molecular oxygen in aqueous solutions. Quantum Northwest qpod-2e cuvette sample compartment was used for temperature control.

Computational Details. Optimized geometry of ground and exited triplet states for all complexes under consideration and their photophysical properties were calculated using the Gaussian 16[1] computer code with DFT methodology. For these purposes, the hybrid Austin-Frisch-Petersson functional with dispersion (APFD)[2] was used due to their best agreement with the experimental results. For all atoms were chosen the Stuttgart-Dresden effective core pseudopotential (SDD) with the corresponding basis set[3]. The Polarizable Continuum Model (PCM)[4] was applied for simulation of effects of water as a non-specific solvent.

Energies of emission were calculated as the difference between the energy of the optimized triplet state and the energy of singlet state at the same triplet geometry (‘vertical’ transition). The electronic absorption spectra were obtained using TD-DFT methodology with 180 excited states for all complexes. The UV/Vis absorption spectra was obtained from previously calculated oscillator strengths using the method described in work[5] with Lorentzian broadening of 2000 cm^{-1}.

The electron density during absorption and emission transitions was investigated using Natural Transition Orbitals (NTO)[6] and Interfragment Charge Transfer (IFCT)[7] calculations.

The Multiwfn 3.6 software[7] was used for both methods. The changes of electronic density Δρ during the $S_0 \rightarrow S_i$ transitions were estimated as:

$$\Delta\rho(S_0 \rightarrow S_i) = \sum_k |\Psi_{ik}(virt)|^2 - \sum_k |\Psi_{ik}(occ)|^2$$

where Ψ_{ik}(occ) and Ψ_{ik}(virt) are NTO pairs for $S_0 \rightarrow S_i$ transition. The electronic density's change during $T_1 \rightarrow S_0$ transition was similarly.

Cell cultures. In vitro studies were performed on the CT26 mouse colorectal cancer cell line. CT26 cells were cultivated according to the standard protocol in complete growth medium DMEM – Dulbecco's Modified Eagle Medium (Gibco, Carlsbad, CA, USA) with 10% FBS – fetal bovine serum (HyClone, USA), glucose (4.5 g/l) (Gibco, Carlsbad, CA, USA) and L-glutamine (Gibco, Carlsbad, CA, USA) at 37°C, 5% CO_2. Cell passage was performed 3 times a week using solutions of Versen (Gibco, Carlsbad, CA, USA) and 0.25% trypsin (Thermo Fisher Scientific, Waltham, MA, USA) when the cell monolayer reached 70–90% of the area of the culture flask.

MTT Assay. CT26 tumor cells were seeded in flat-bottomed 96-well plates (1 x 10^3 cells per well in 200 µl of DMEM). The complexes were added to the cells at a concentration of 0–150 µM and incubated for 24 h, after which the cells were treated with the MTT reagent 3(4,5-dimethyl-2-thiazolyl)-2,5-diphenyl-2H-tetrazol bromide (Alfa Aesar, Haverhill, MA, USA) at a concentration of 0.5 mg/ml according to the manufacturer's protocol. Cells were incubated with the reagent solution at 37°C in 5% CO_2 for 2 h. The formed formazan crystals were dissolved in 100 µl of DMSO and the absorbance was measured from the wells spectrophotometrically on a multimodal plate reader (Synergy Mx; BioTek Instruments, Winooski, VT, USA). For each well, the percentage of viable cells relative to the control was determined. For each concentration of the complex, 3 replications of 10 wells were performed.

Cell compartment staining. To determine the subcellular localization of the complexes, cells were seeded in 35 mm glass bottom FluoroDish dishes (Ibidi GmbH, Gräfelfing, Germany) at 3×105 cells in 2 ml of DMEM. After cell adhesion, the monolayer was washed with a PBS solution and incubated with **Ir2** and **Ir3** probes solutions (100 µM) for 3 hours, after which the cell monolayer was washed with a PBS solution. Lysosomes were stained with LysoTracker Red

DND-99 ((Thermo Fisher Scientific, Waltham, MA, USA)) at a concentration of 3 μM, mitochondria were stained with MitoTracker 405 Blue (Thermo Fisher Scientific, Waltham, MA, USA) was used at the concentration of 50 nM, according to the manufacturer's protocol for 1 hour.

Confocal microscopy and colocalization assay. Microscopic studies were carried out on a laser-scanning microscope LSM 880 (Carl Zeiss, Berlin, Germany), equipped with a TCSPC-based module (two hybrid detectors, HPM-100-40; two single-photon counting cards, SPC-150; Becker & Hickl GmbH, Berlin, Germany) and a Ti:Sa femtosecond laser MaiTai HP (Spectra-Physics Inc., Milpitas, CA, USA). The images were obtained using a water-immersion lens C-Apochromat 40×/1.2 NA. Luminescence of **Ir2** and **Ir3** was excited with a Ti:Sa laser at a wavelength of 750 nm, the emission was detected in the range 500–570 nm. The fluorescence of the lysotracker dye was excited at 633 nm and a fluorescence signal was detected in the range of 660-680 nm, the mitotracker fluorescence was excited at 405 nm and a fluorescence signal was detected in the range of 420-470 nm. The colocalization of the complexes and organelle-specific dyes was assessed in ImageJ software (National Institutes of Health, Bethesda, MY, USA) using the Jacob plugin to determine the Mander's coefficient M1. Quantification of luminescence intensity of **Ir2** and **Ir3** was performed in the cell cytoplasm by manual selection of the cytoplasm as region of interest. Calculations were made for 30-50 cells in total from 5 fields of view for every time point. Dead cells identified by round morphology on the bright-field images were excluded from the analysis. Results are presented as mean ± standard deviation.

PLIM. Phosphorescence lifetime imaging microscopy (PLIM) was performed using LSM880 laser-scanning microscope, equipped with TCSPC module SPC-150 (Becker & Hickl GmbH, Germany). Phosphorescence was excited in two-photon mode using a Ti:Sa femtosecond laser MaiTai HP (Spectra-Physics, USA) at 750 nm with 80 MHz repetition rate and 140 fs pulse width, the emission was detected in the range 500-720 nm using the HPM-100-40 Hybrid Detector (Becker & Hickl GmbH, Germany). Images were collected with an oil immersion objective lens C Plan-Apochromat 40x/1.3 NA. Scanning was performed at a frame time of 17.275 s, corresponding to a pixel dwell time 65.9 μs, time range of PLIM recording was 19.20 μs, the total acquisition time was 120 s. Image size was 512x512 pixels.

PLIM images were processed using SPCImage 8.5 software (Becker & Hickl GmbH, Germany). The phosphorescence decay curves were fitted with a monoexponential decay model with an average goodness of the fit $0.8 \leq \chi^2 \leq 1.2$. The average number of photons per curve were not less than 5000 at binning 10. The data are presented as mean phosphorescence lifetime per cell.

NMR and ESI HRMS data

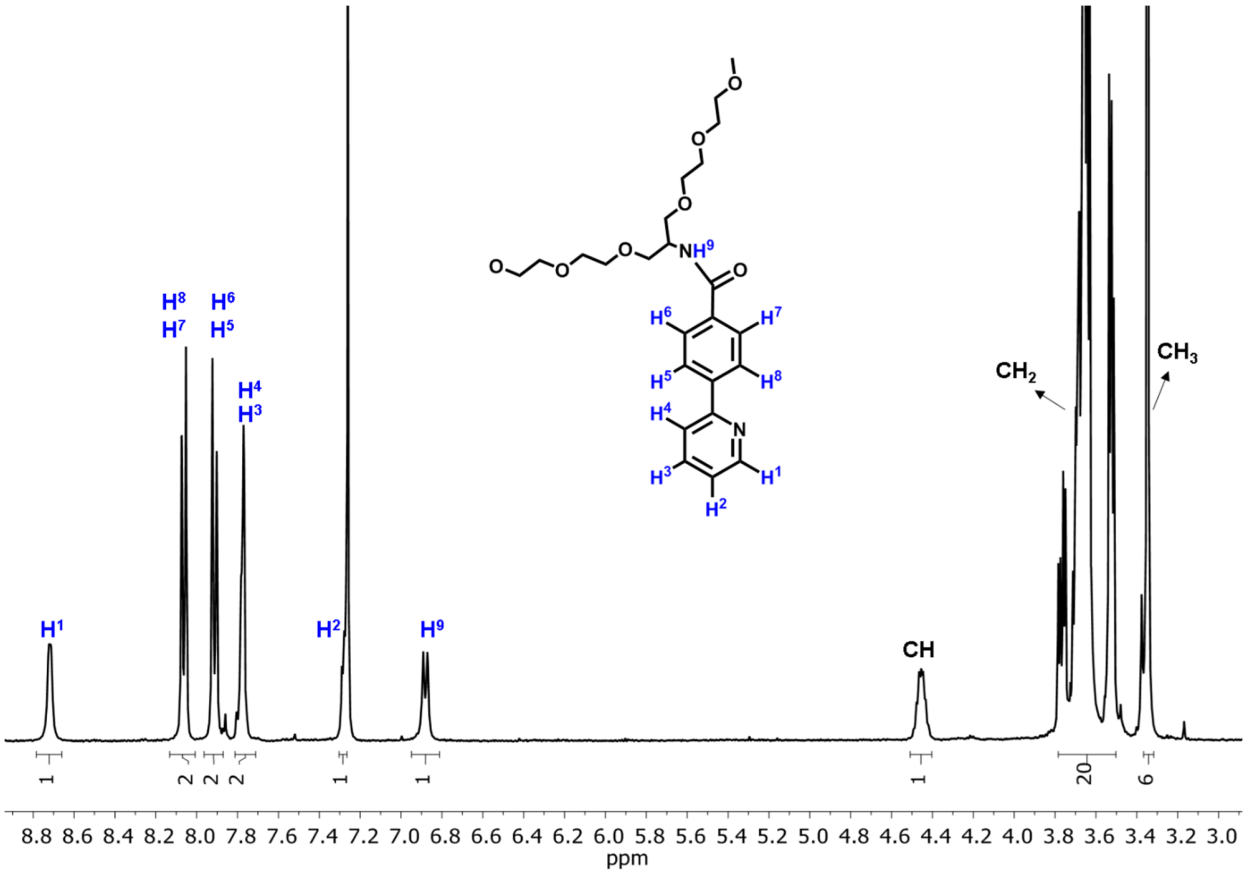

Figure S1. ^{1}H NMR spectrum of **N^C**, $CDCl_3$, 298 K.

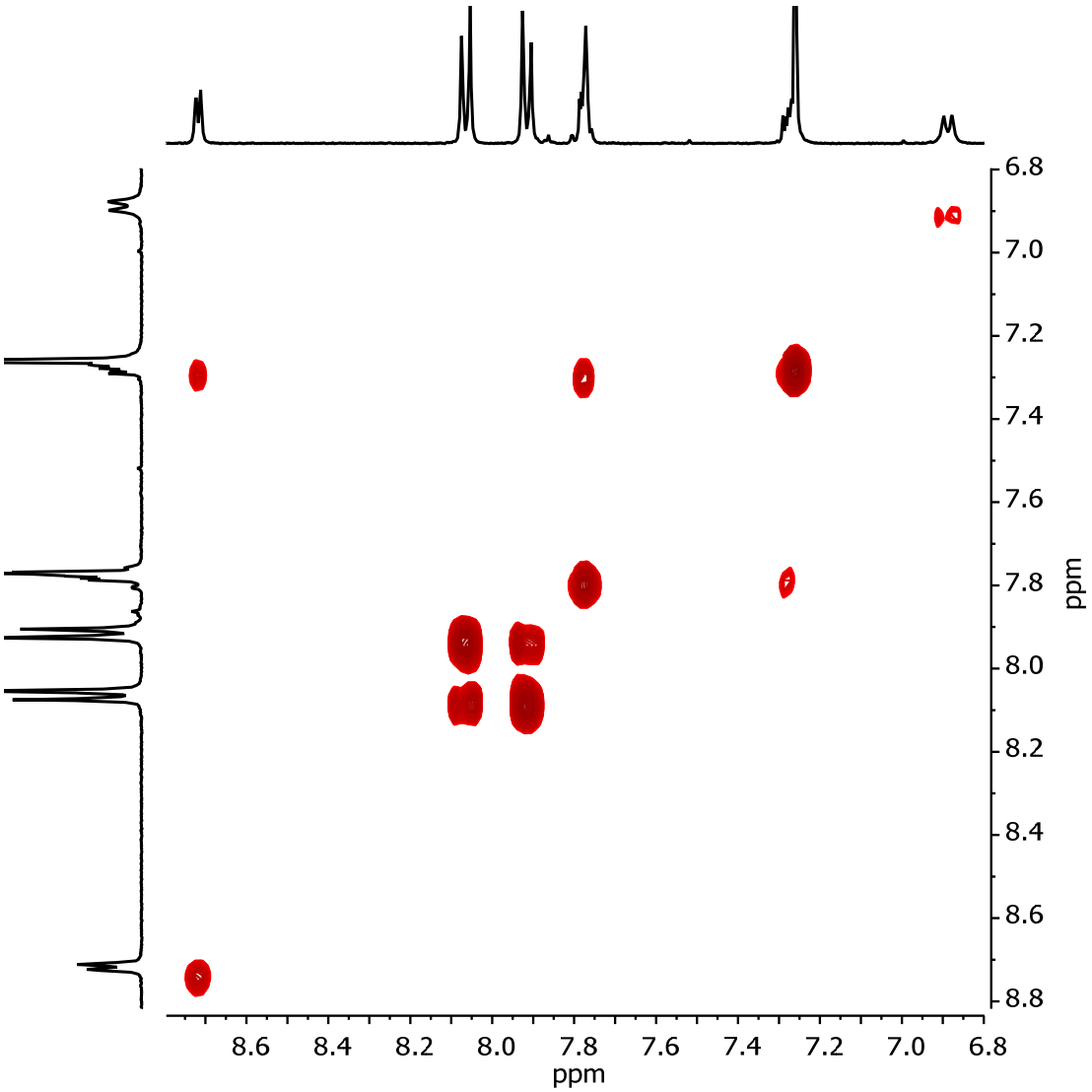

Figure S2. ^{1}H-^{1}H COSY NMR spectra of **N^C**, $CDCl_3$, 298 K.

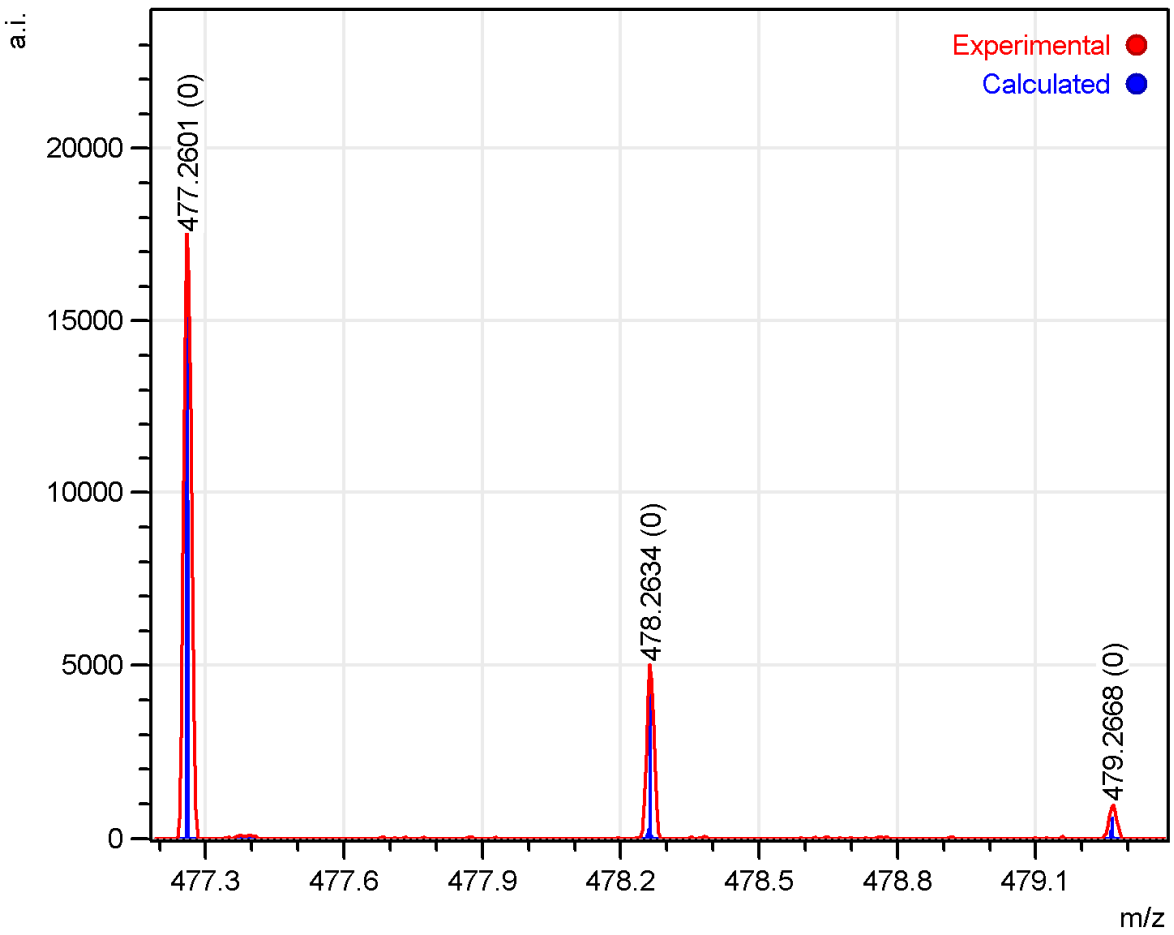

Figure S3. ESI$^+$ mass-spectrum of **N^C** ([M+H]$^+$cation area), solvent – methanol.

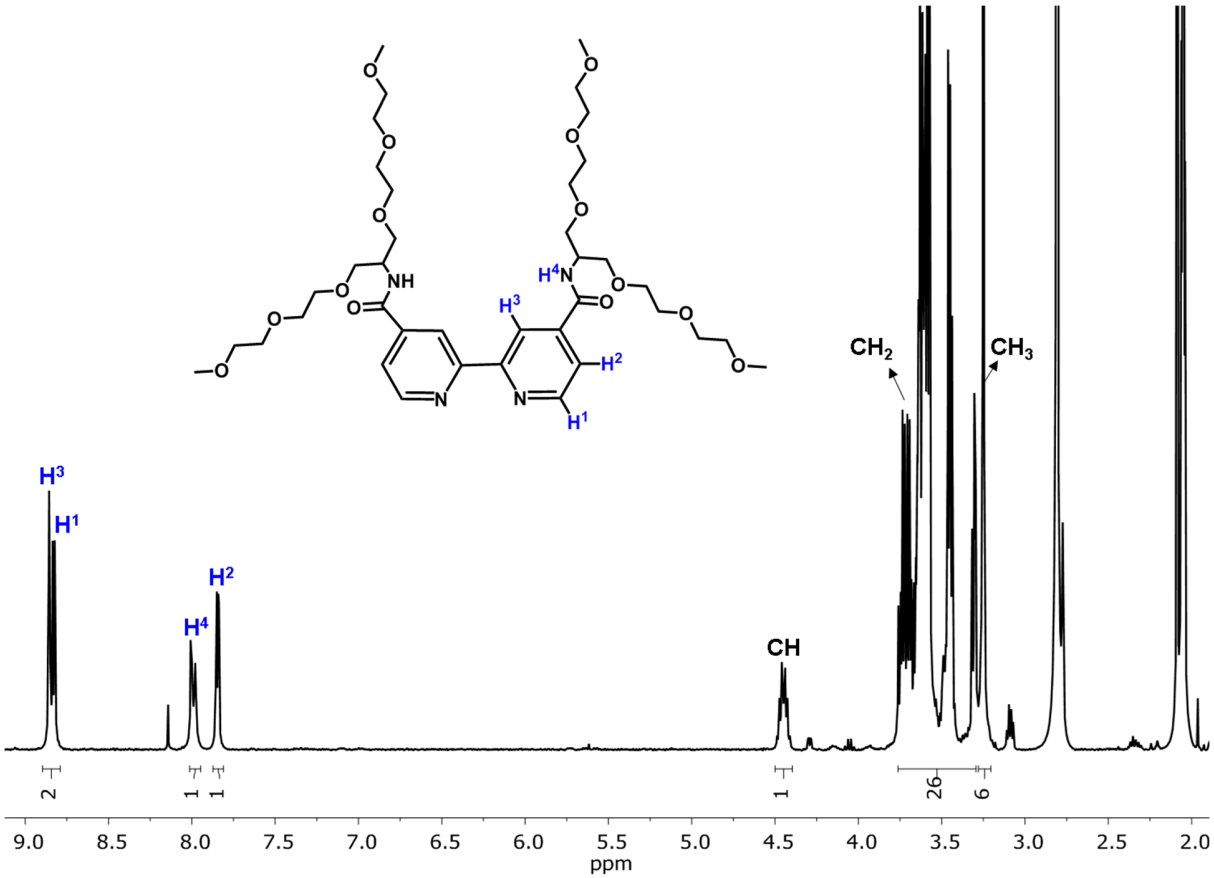

Figure S4. ^{1}H NMR spectrum of **N^N1**, $(CD_3)_2CO$, 298 K.

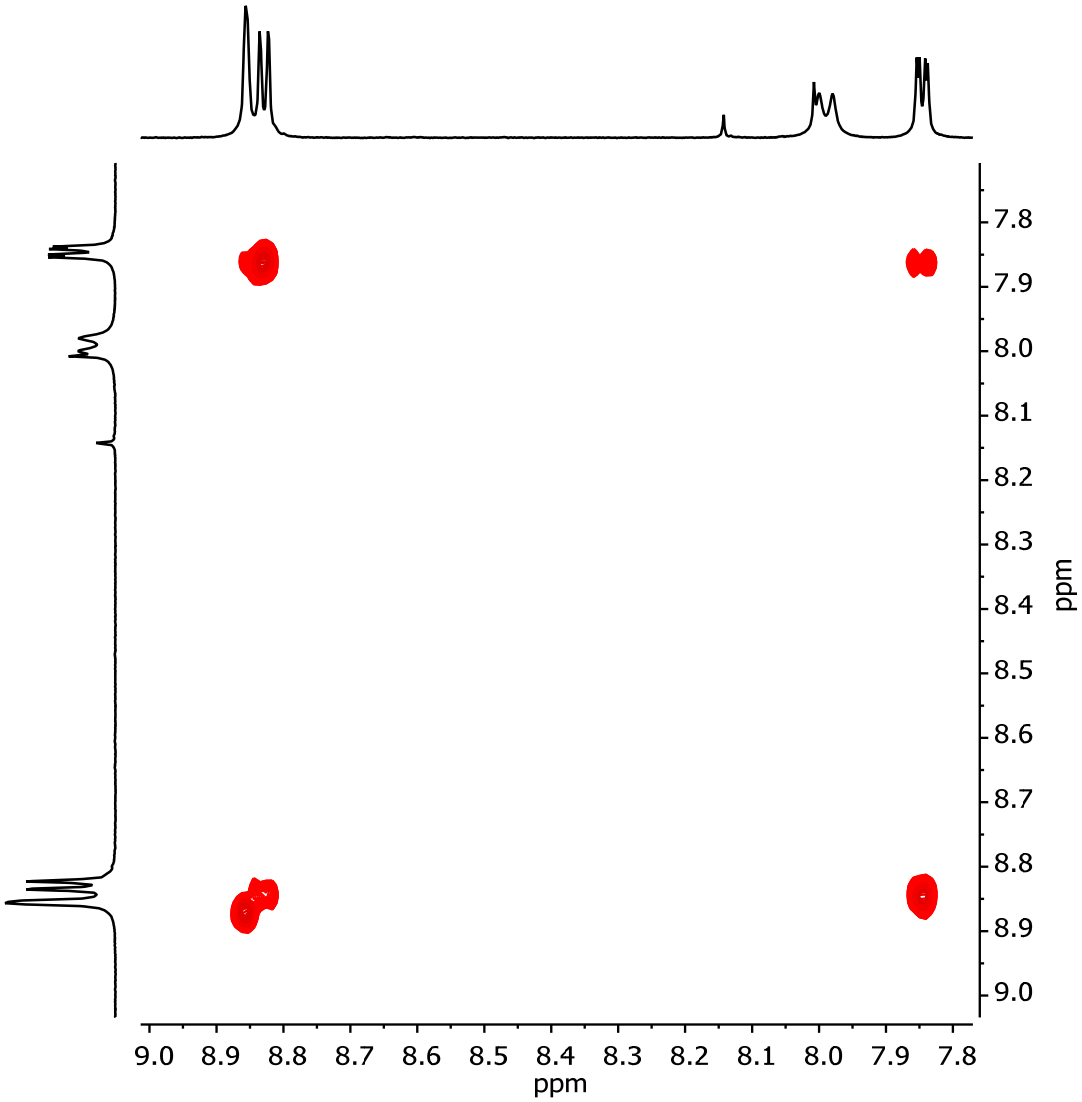

Figure S5. ^{1}H-^{1}H COSY NMR spectra of **N^N1**, $(CD_3)_2CO$, 298 K.

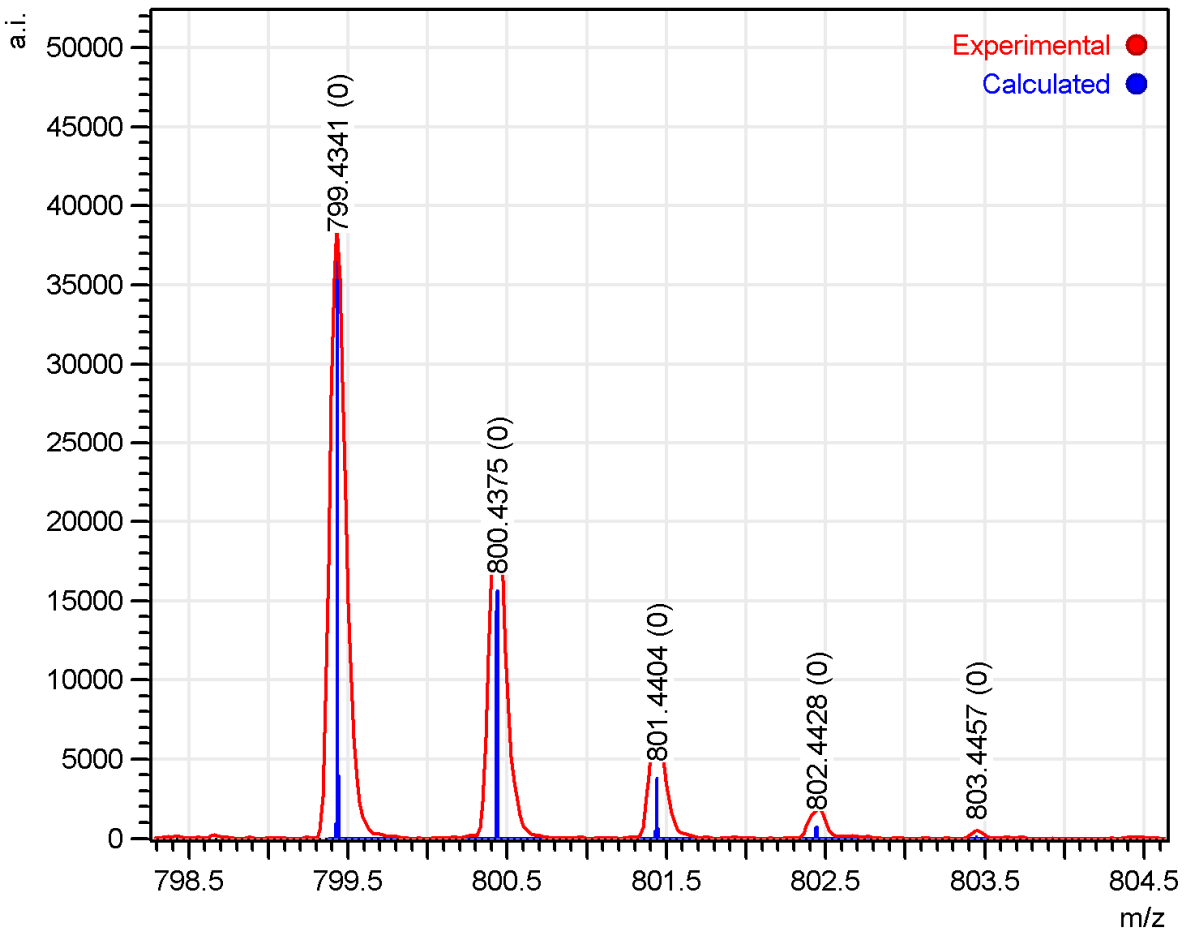

Figure S6. ESI$^+$ mass-spectrum of **N^N1** ([M+H]$^+$cation area), solvent – methanol.

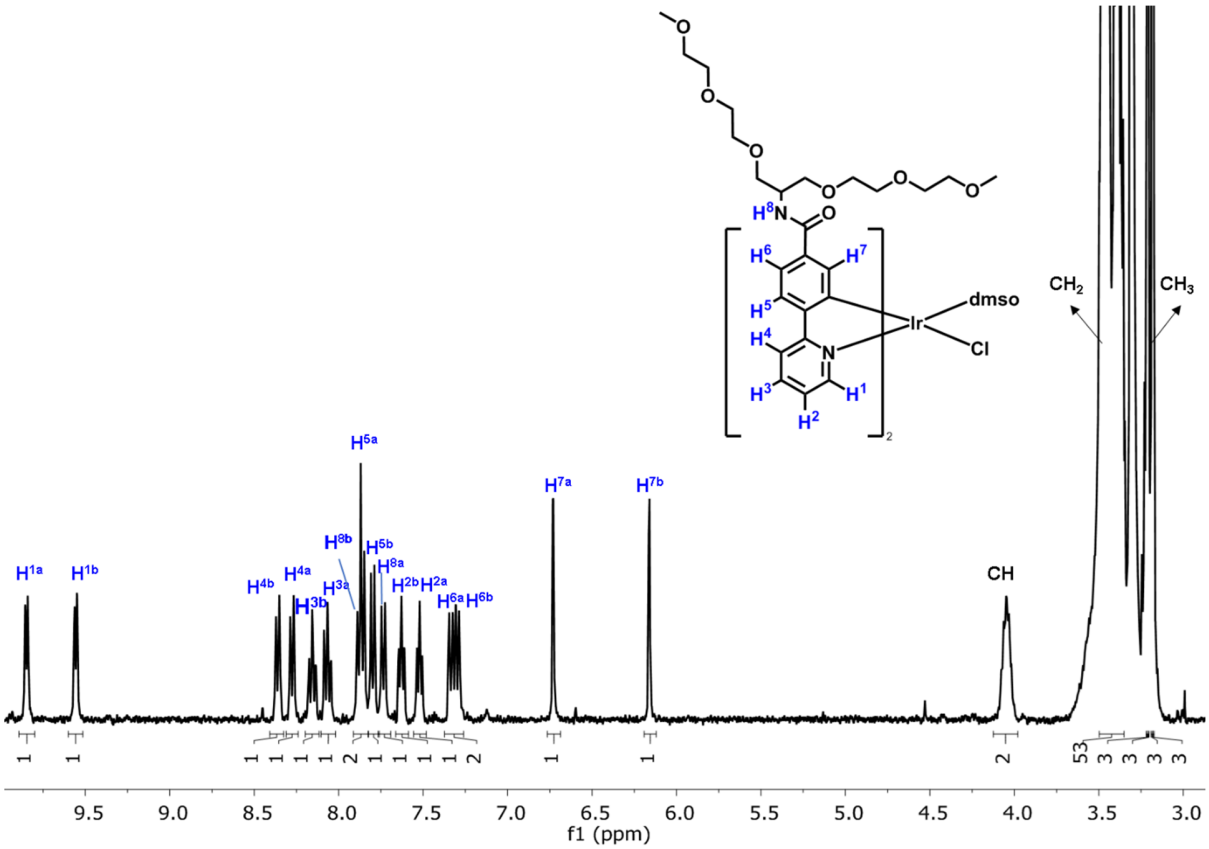

Figure S7. ^{1}H NMR spectrum of dissociated dimer $[Ir_2(N\hat{}C)_4Cl_2]$, $(CD_3)_2SO$, 298 K.

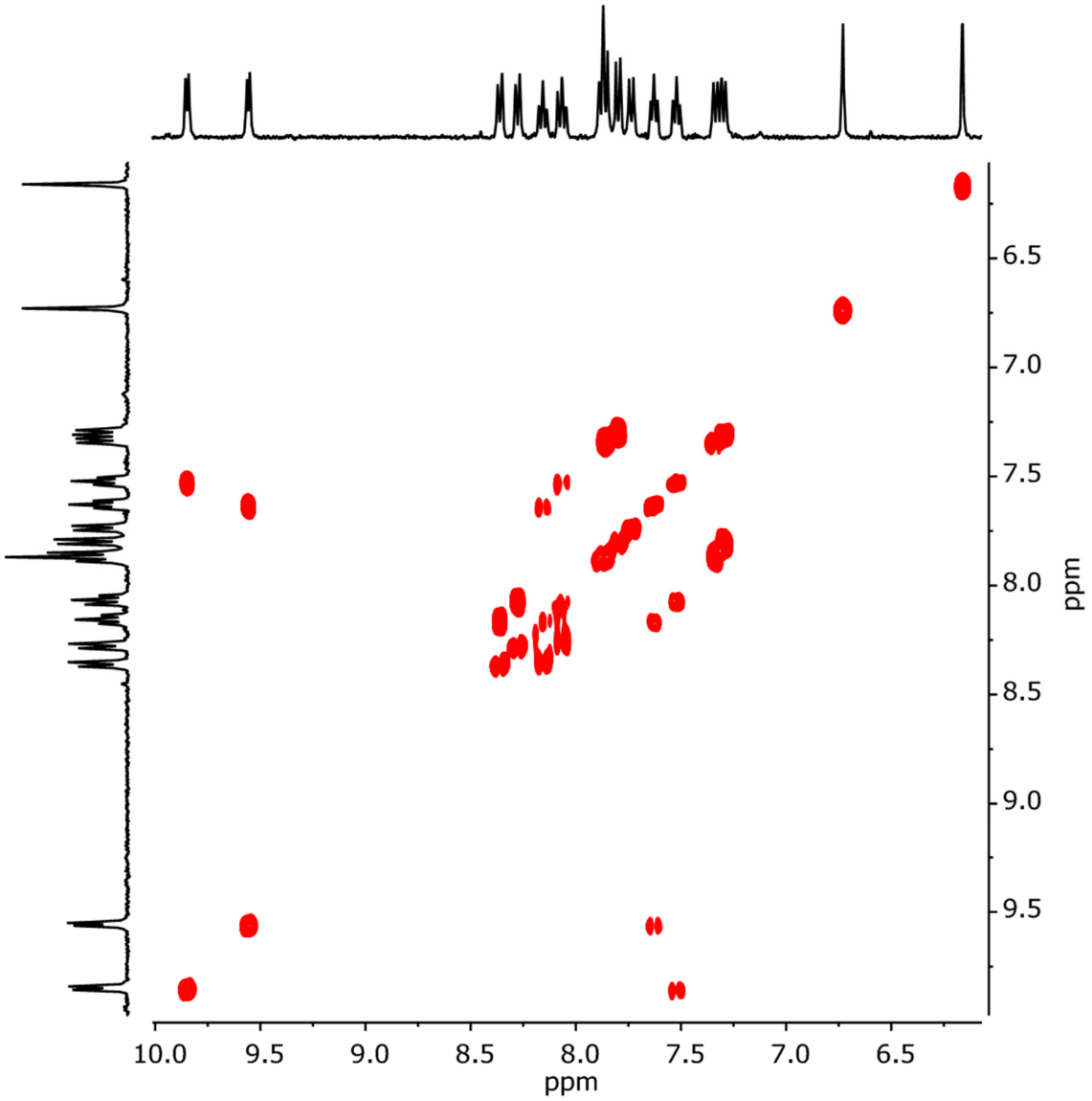

Figure S8. ^{1}H-^{1}H COSY NMR spectra of dissociated dimer [$Ir_2(N^C)_4Cl_2$], $(CD_3)_2SO$, 298 K.

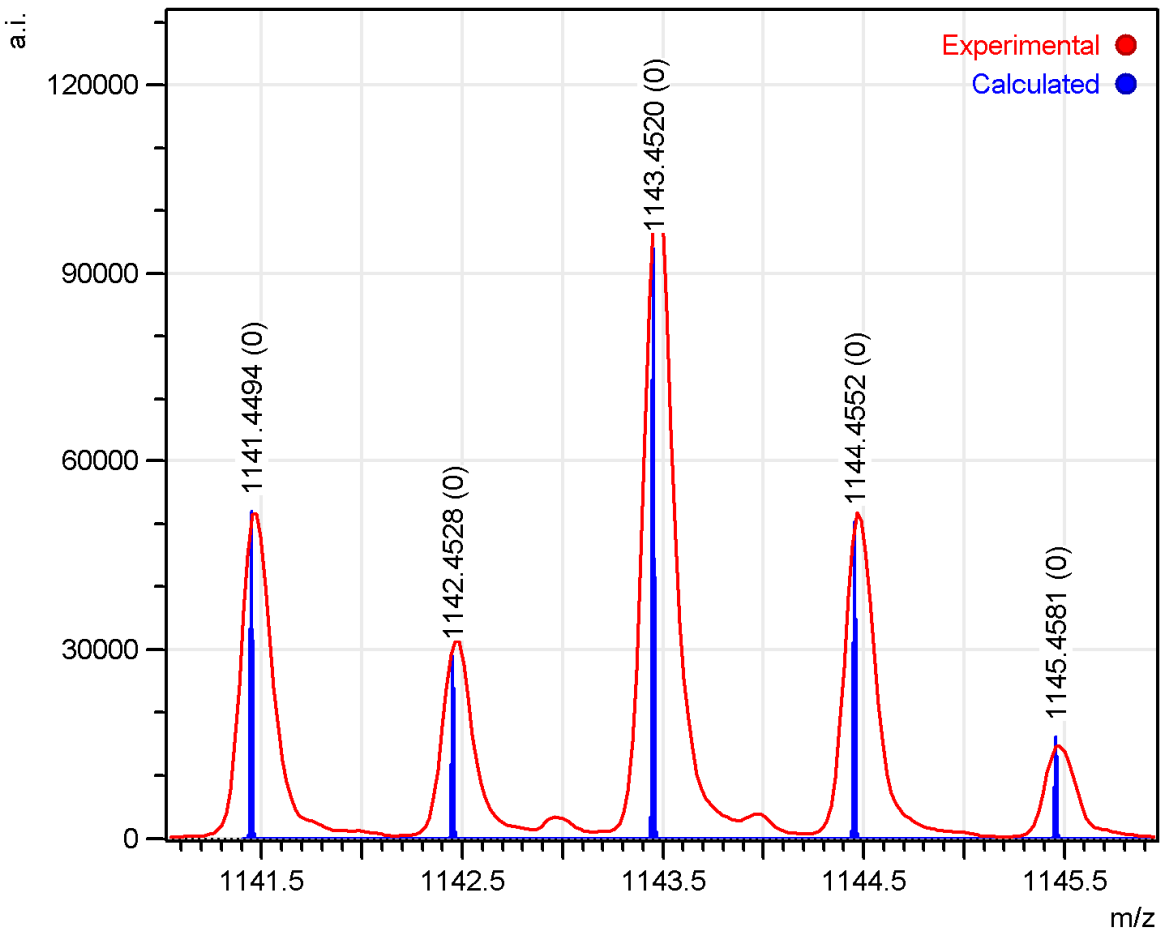

Figure S9. ESI^+ mass-spectrum of dimer $[Ir_2(N^C)_4Cl_2]$ ($[Ir(N^C)_2]^+$cation area), solvent – methanol.

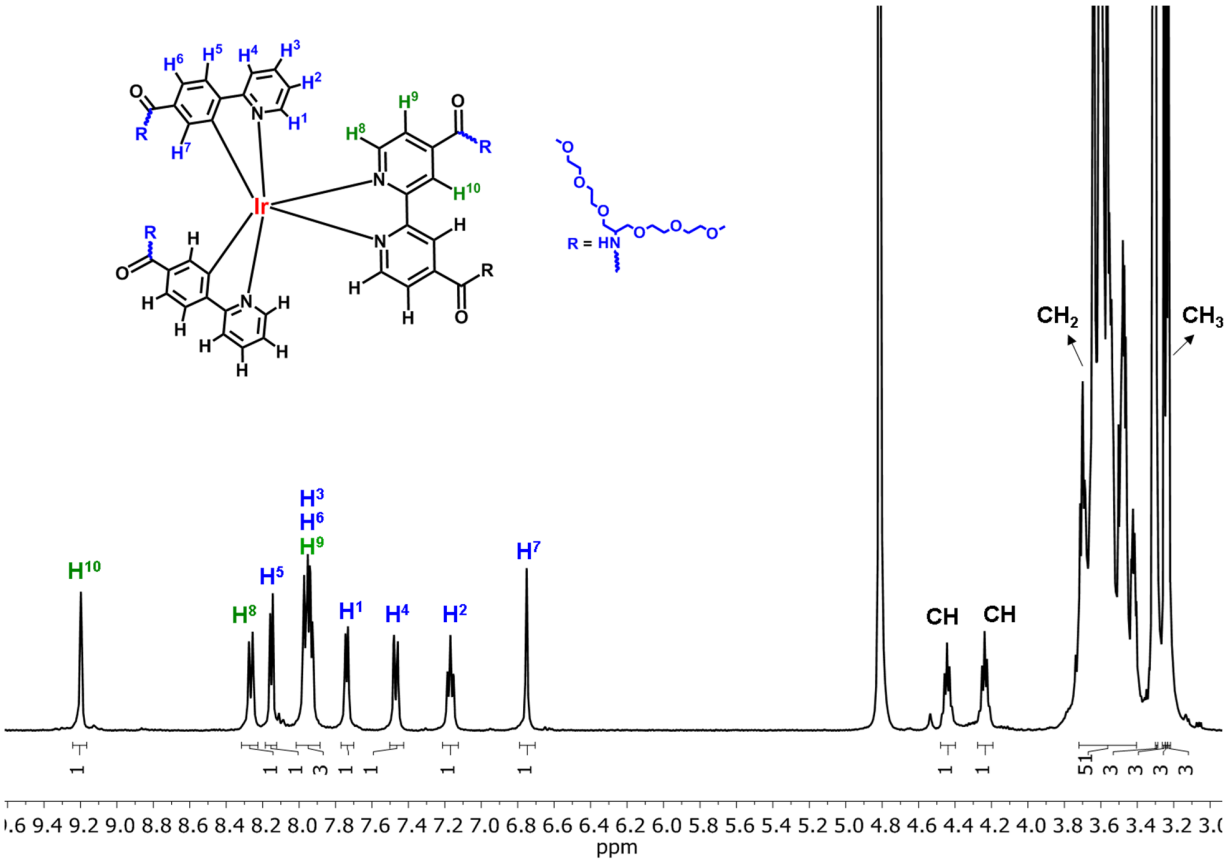

Figure S10. ^{1}H NMR spectrum of **Ir1**, CD_3OD, 298 K.

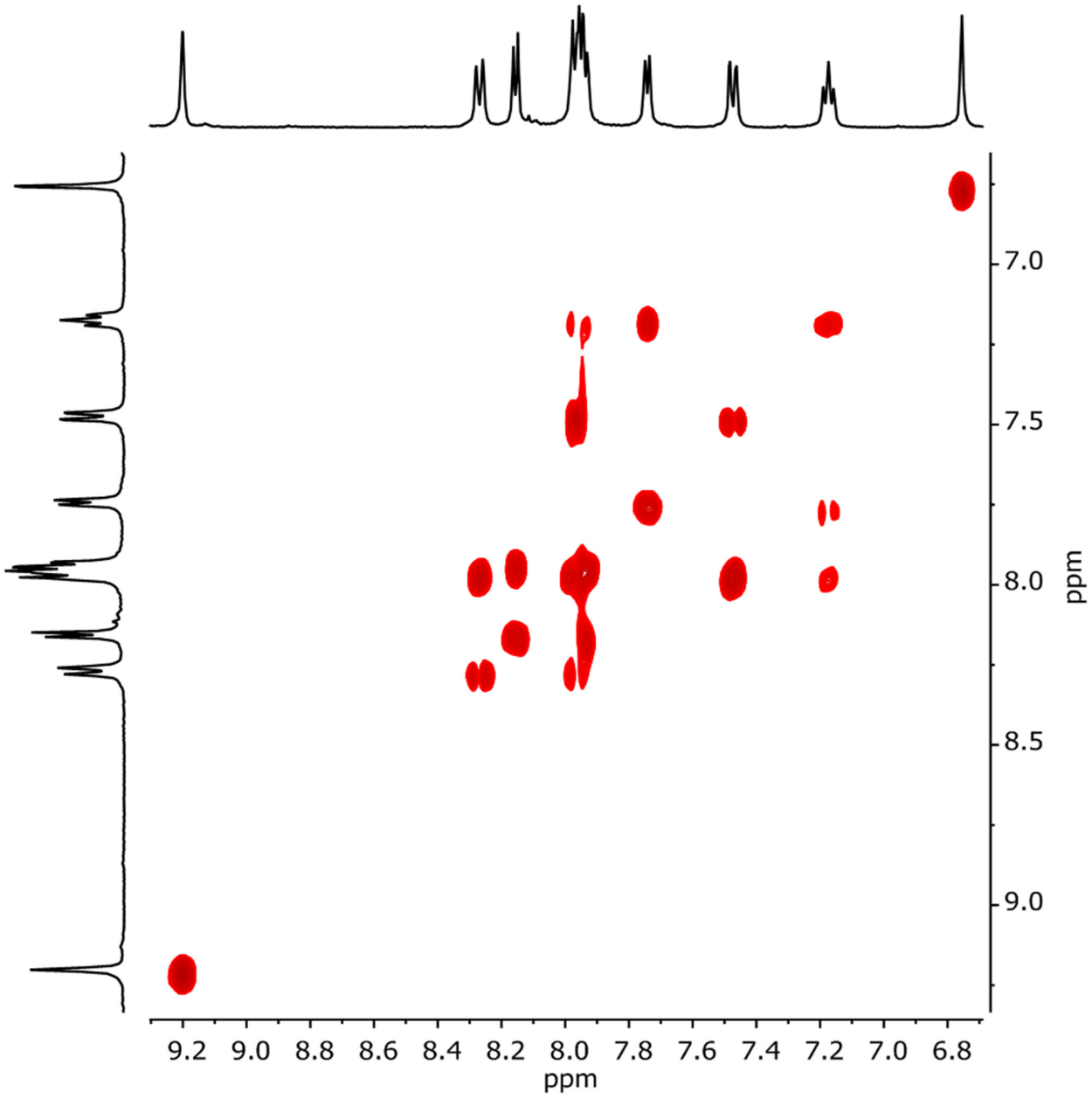

Figure S11. ^{1}H-^{1}H COSY NMR spectra of **Ir1**, CD_3OD, 298 K.

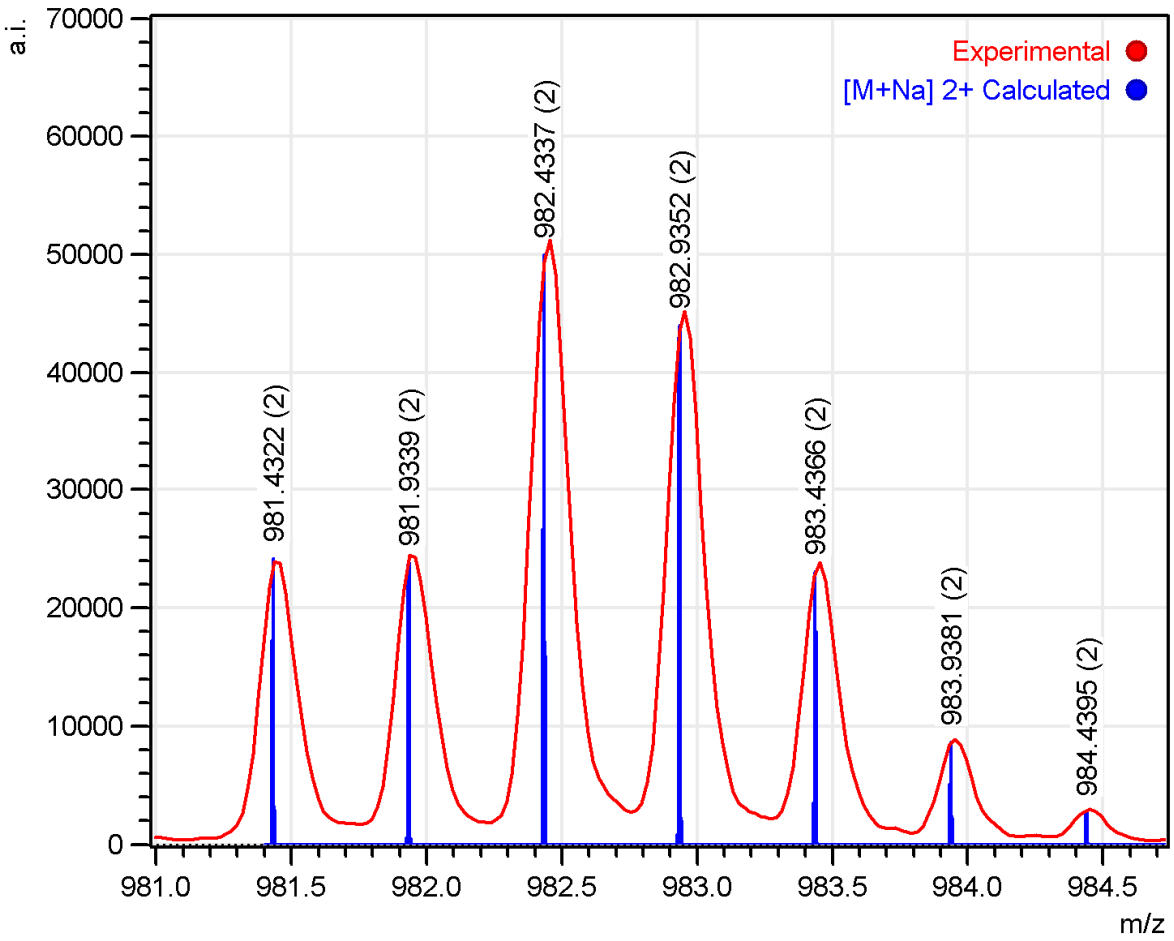

Figure S12. ESI^{+} mass-spectrum of **Ir1** ([M+Na]$^{2+}$cation area), solvent – methanol.

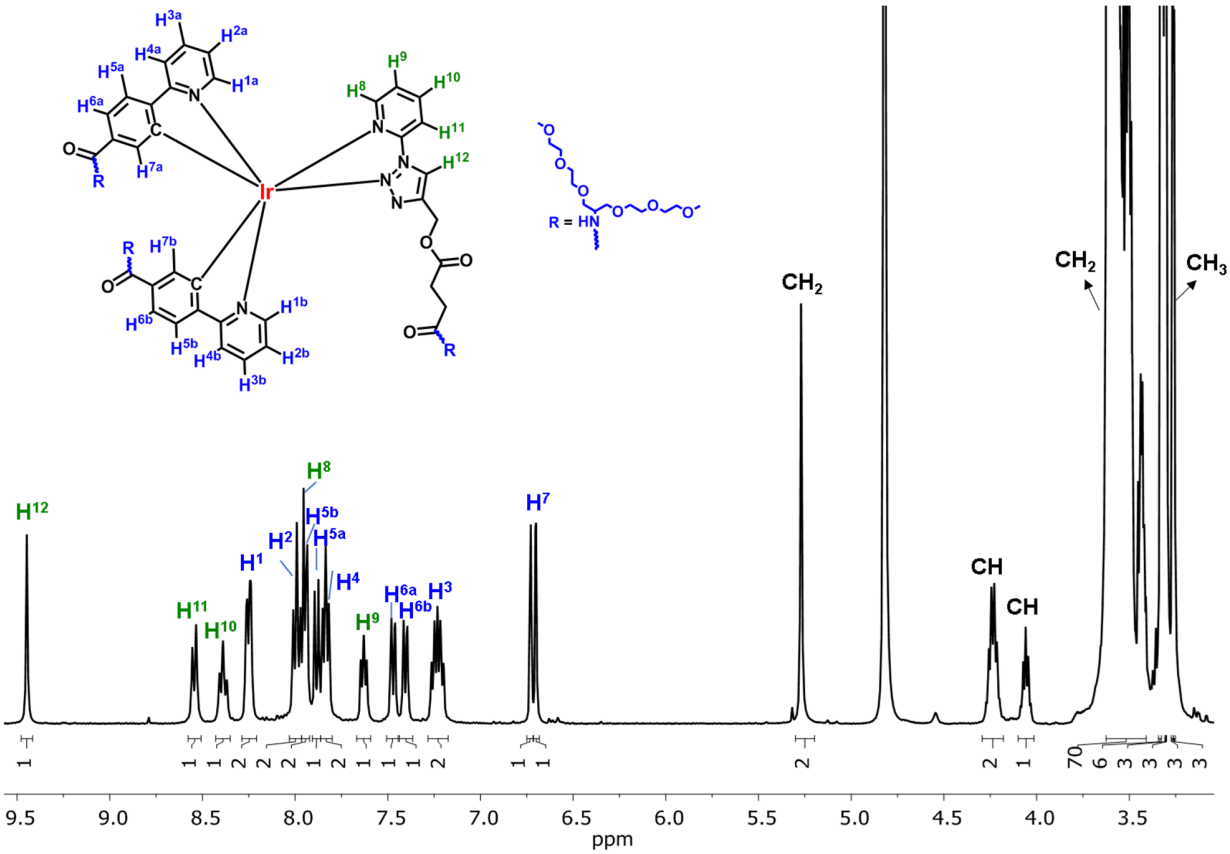

Figure S13. ^{1}H NMR spectrum of **Ir2**, CD_3OD, 298 K.

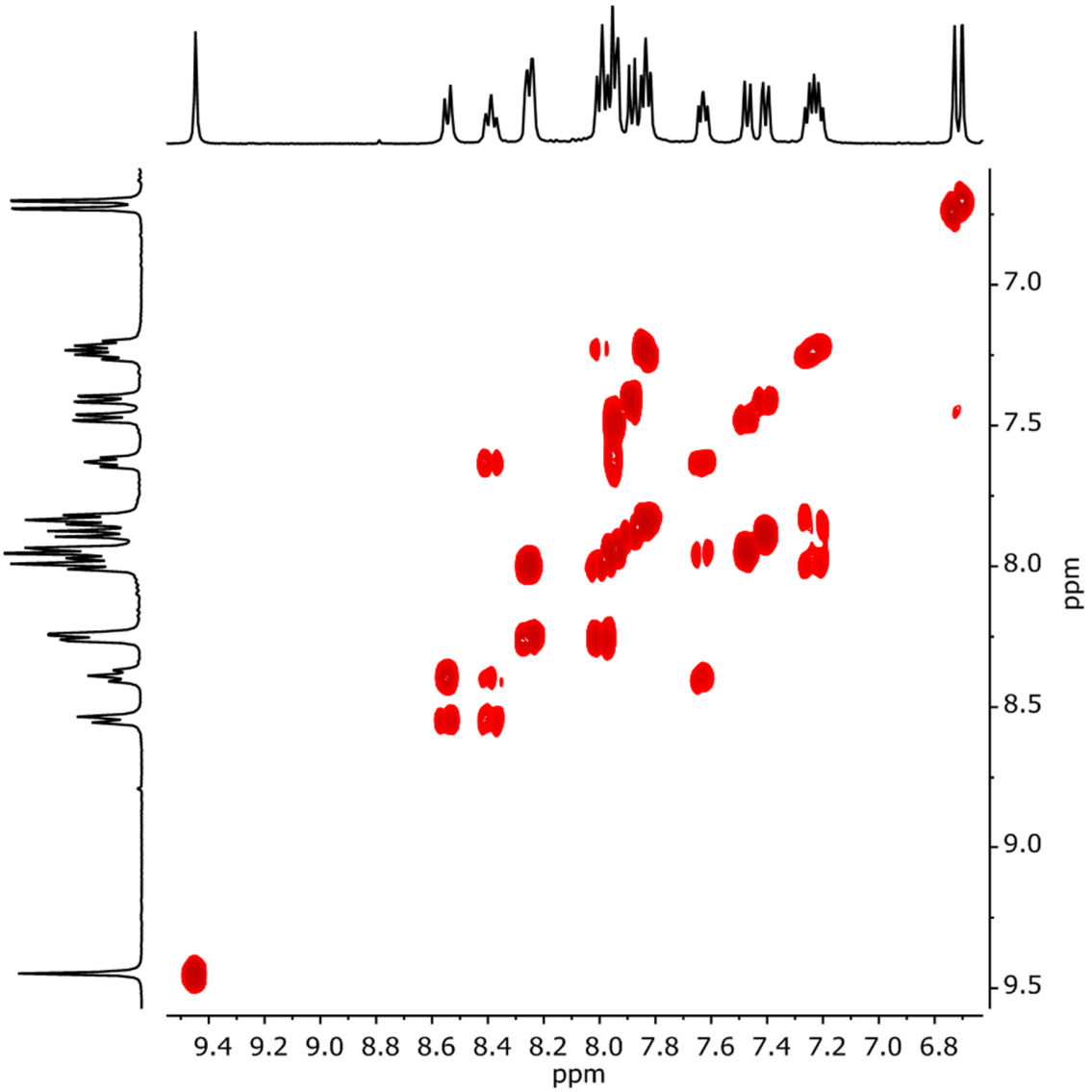

Figure S14. ^{1}H-^{1}H COSY NMR spectra of **Ir2**, CD_3OD, 298 K.

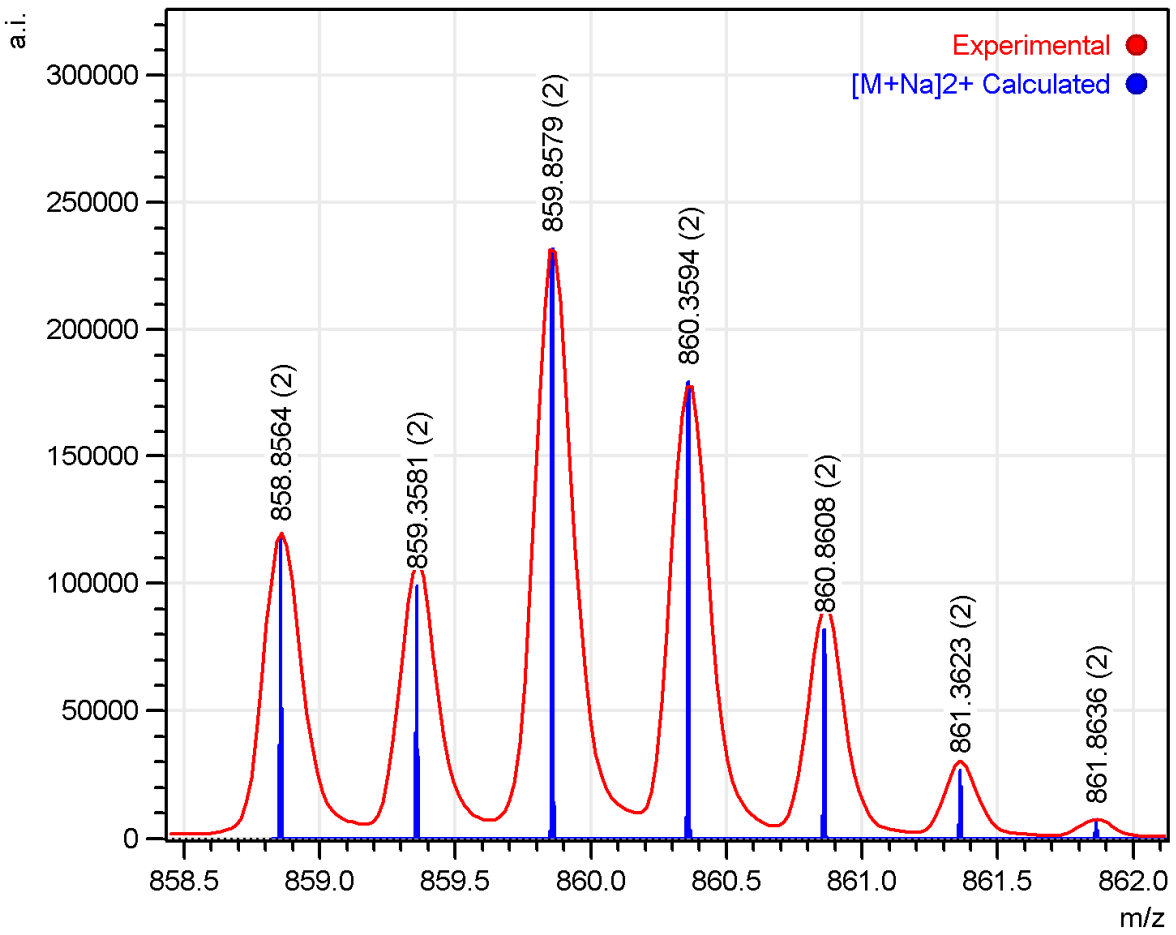

Figure S15. ESI^+ mass-spectrum of **Ir2** ($[M+Na]^{2+}$cation area), solvent – methanol.

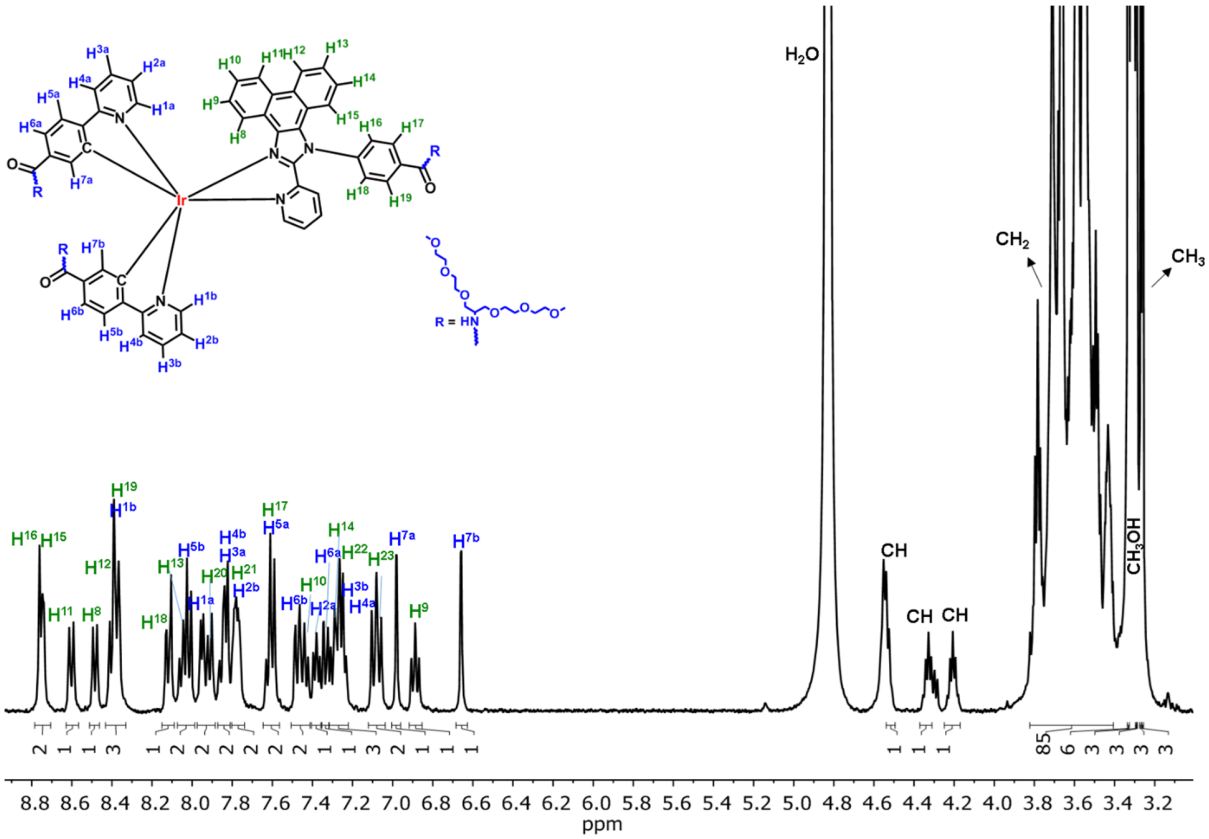

Figure S16. ^{1}H NMR spectrum of **Ir3**, CD_3OD, 298 K.

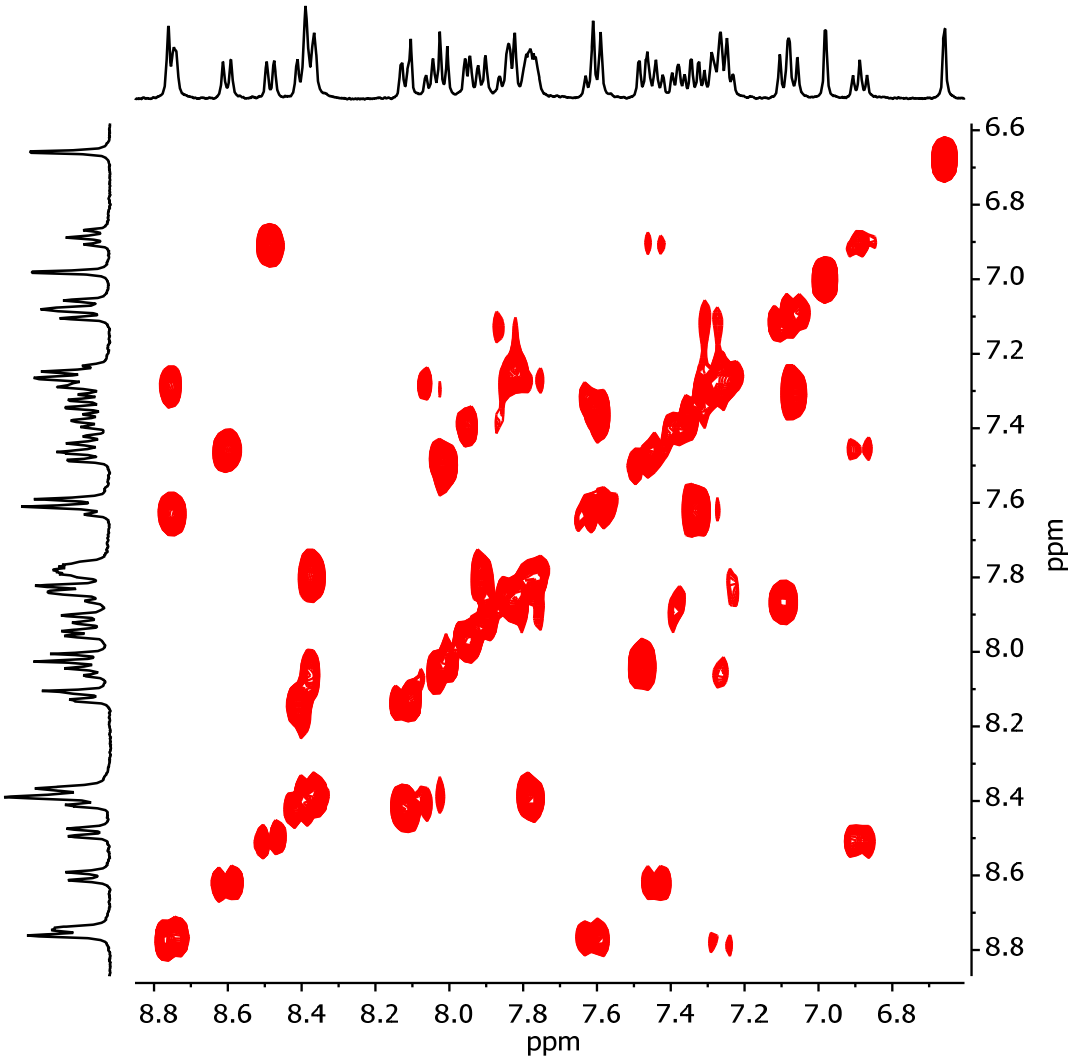

Figure S17. ^{1}H-^{1}H COSY NMR spectra of **Ir3**, CD_3OD, 298 K.

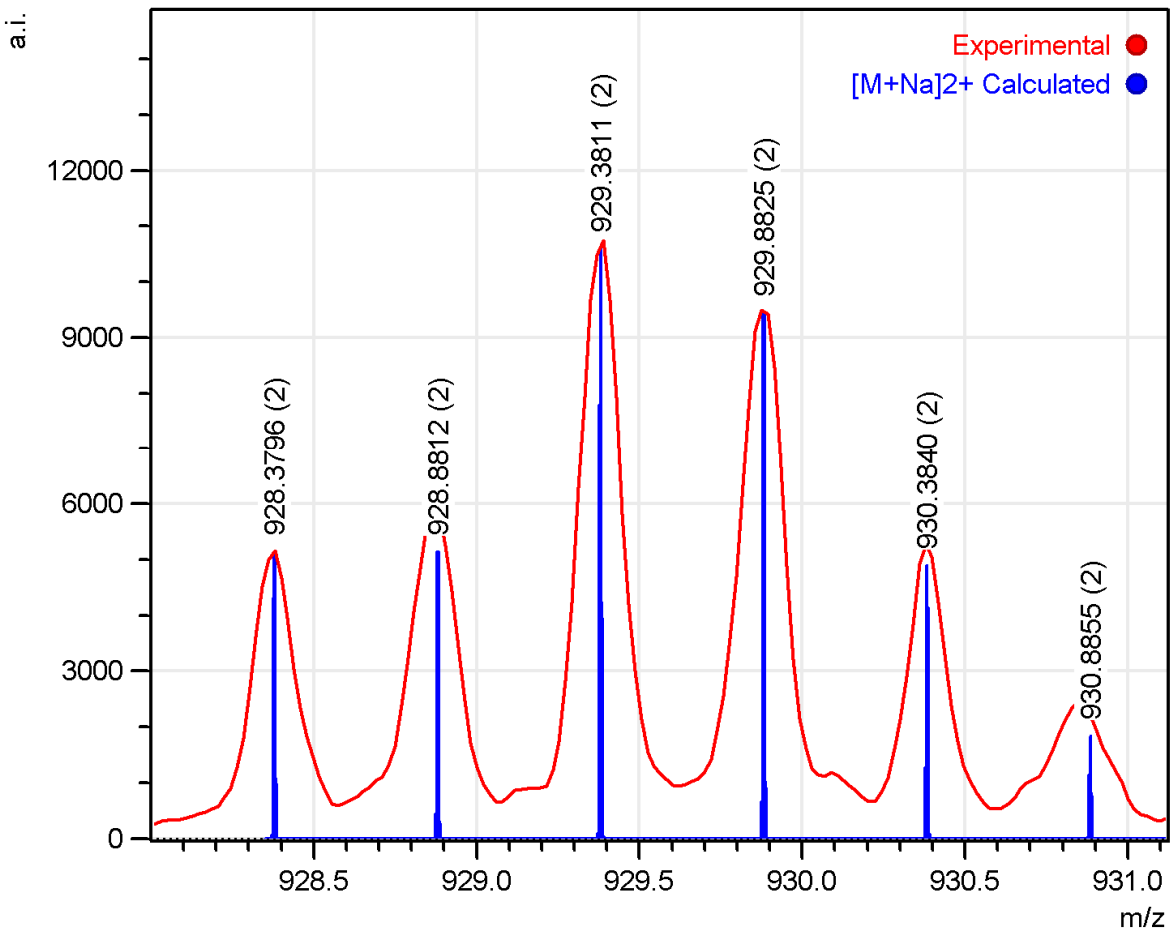

Figure S18. ESI^{+} mass-spectrum of **Ir3** ([M+Na]$^{2+}$cation area), solvent – methanol.

Photophysical data

Table S1. Values of excitation state lifetime of complexes **Ir2** and **Ir3** in various aqueous media and at different oxygen concentrations. Excitation at 355 nm, T = 37°C, C(Complex) = 10 μM.

Complex	Water		0.01M PBS		DMEM + 10% FBS	
	$C(O_2)$, μM	τ, ns	$C(O_2)$, μM	τ, ns	$C(O_2)$, μM	τ, ns
Ir2	215	683	204	701	200	878
	163	816	147	861	154	1018
	99	1102	56.2	1397	119	1155
	39.1	1617	28.1	1723	75.7	1403
	15.2	2014	10.8	1988	27.2	1852
	4.93	2182	0.95	2195	2	2213
Ir3	216	1221	206	1239	200	1560
	133	1696	179	1365	168	1741
	67.4	2390	127	1693	123	2084
	39.7	3004	83.9	2177	86.4	2471
	12.7	3878	14	3791	43.9	3137
	3.89	4214	4.04	4220	3.22	4215

Computational data

Table S2. Calculated and experimental wavelength of emission maxima of complexes **Ir1-Ir3**.

Complex	Calculated wavelength, nm	Experimental wavelength, nm
Ir1	665	651
Ir2	554	502, 535, 575sh
Ir3	557	543sh, 573

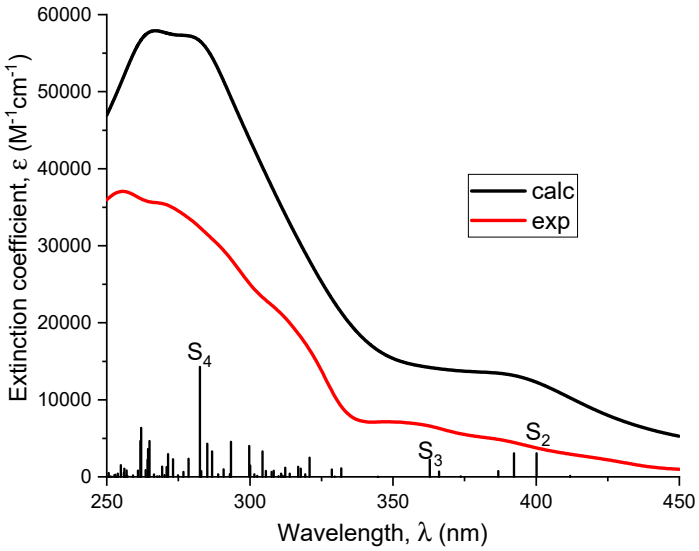

Figure S19. Absorption spectra of **Ir1**: experimental (red) and calculated (black) lines with oscillator strengths of electronic transitions (bars).

Table S3. Calculated absorption maxima (λ) and oscillator strengths (f) of complex **Ir1**.

Transitions	λ_{abs}, nm	*f*	Contribution of main NTO pair in transition (%)
S_0-S_4	283	0.39	49
S_0-S_3	363	0.06	50
S_0-S_2	400	0.08	95
S_0-S_1	517	0.00	98

Table S4.The decrease (violet) and increase (terracotta) of electron density for most intensive electronic absorption transitions of **Ir1**. The data for the corresponding interfragment charge transfer (IFCT) are given below the figures. Diagonal values represent intraligand transitions, off-diagonal values represent a charge transfer from “Donor” to “Acceptor”.

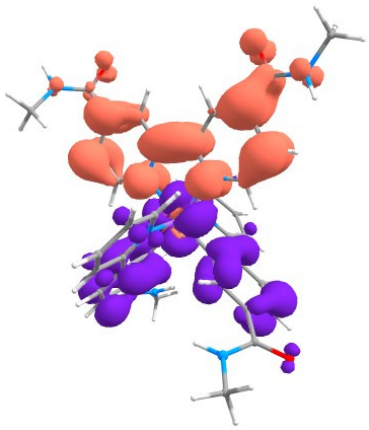

$S_0 \rightarrow S_1$

Donor	Acceptor			
	Ir	N^N1	N^C	N^C’
Ir	0.010	0.370	0.002	0.003
N^N1	0.001	0.021	0.000	0.000
N^C	0.008	0.285	0.002	0.002
N^C’	0.008	0.285	0.002	0.002

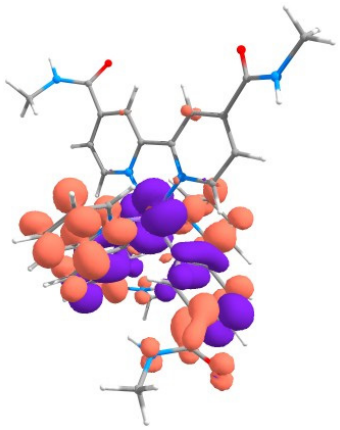

$S_0 \rightarrow S_2$

Donor	Acceptor			
	Ir	N^N1	N^C	N^C’
Ir	0.007	0.018	0.177	0.184
N^N1	0.000	0.001	0.010	0.011
N^C	0.005	0.014	0.136	0.141
N^C’	0.005	0.014	0.136	0.141

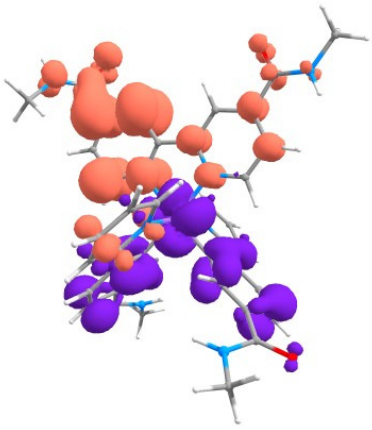

$S_0 \rightarrow S_3$

Donor	Acceptor			
	Ir	N^N1	N^C	N^C’
Ir	0.005	0.299	0.006	0.018
N^N1	0.001	0.038	0.001	0.002
N^C	0.005	0.289	0.006	0.017
N^C’	0.005	0.287	0.005	0.017

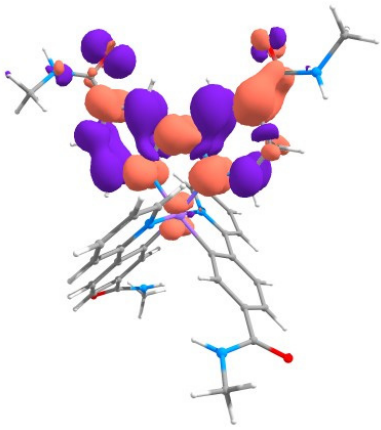

$S_0 \rightarrow S_4$

Donor	Acceptor			
	Ir	N^N1	N^C	N^C’
Ir	0.003	0.135	0.003	0.014
N^N1	0.012	0.549	0.013	0.057
N^C	0.002	0.082	0.002	0.008
N^C’	0.002	0.105	0.002	0.011

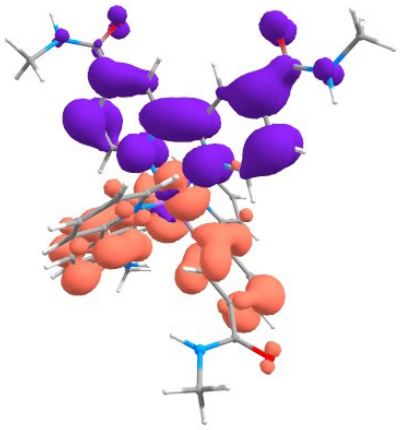

$T_1 \rightarrow S_0$

Donor	Acceptor			
	Ir	N^N1	N^C	N^C’
Ir	0.011	0.001	0.010	0.010
N^N1	0.340	0.025	0.297	0.292
N^C	0.002	0.000	0.002	0.002
N^C’	0.002	0.000	0.002	0.002

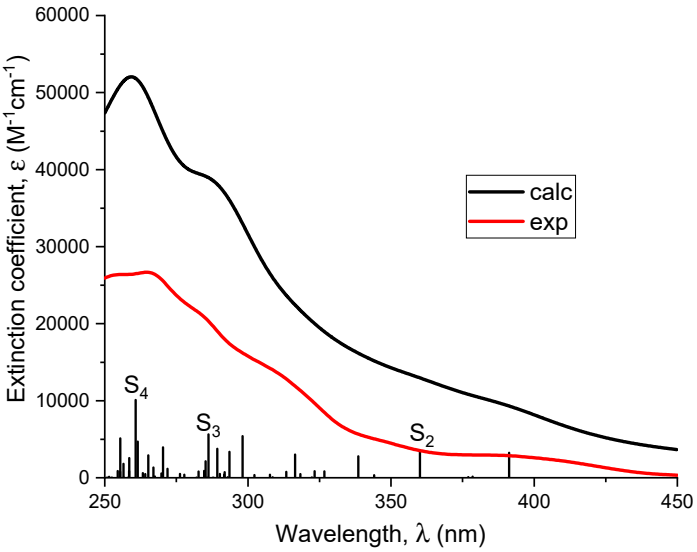

Figure S20. Absorption spectra of **Ir2**: experimental (red) and calculated (black) lines with oscillator strengths of electronic transitions (bars).

Table S5. Calculated absorption maxima (λ) and oscillator strengths (f) of complex **Ir2**.

Transitions	λ_{abs}, nm	*f*	Contribution of main NTO pair in transition (%)
S_0-S_4	261	0.27	52
S_0-S_3	286	0.15	55
S_0-S_2	360	0.10	95
S_0-S_1	462	0.00	98

Table S6.The decrease (violet) and increase (terracotta) of electron density for most intensive electronic absorption transitions of **Ir2**. The data for the corresponding interfragment charge transfer (IFCT) are given below the figures. Diagonal values represent intraligand transitions, off-diagonal values represent a charge transfer from "Donor" to "Acceptor".

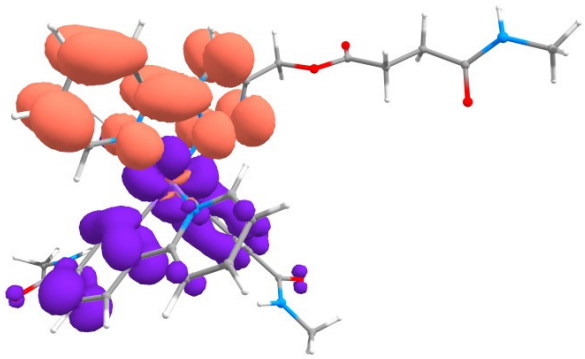

$S_0 \rightarrow S_1$

Donor	Acceptor			
	Ir	N^N2	N^C	N^C'
Ir	0.012	0.336	0.004	0.003
N^N2	0.001	0.020	0.000	0.000
N^C	0.009	0.271	0.003	0.002
N^C'	0.011	0.322	0.004	0.003

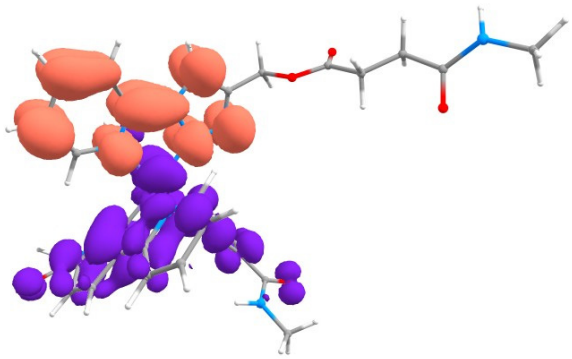

$S_0 \rightarrow S_2$

Donor	Acceptor			
	Ir	N^N2	N^C	N^C'
Ir	0.010	0.288	0.003	0.002
N^N2	0.002	0.053	0.001	0.000
N^C	0.012	0.331	0.004	0.003
N^C'	0.010	0.277	0.003	0.002

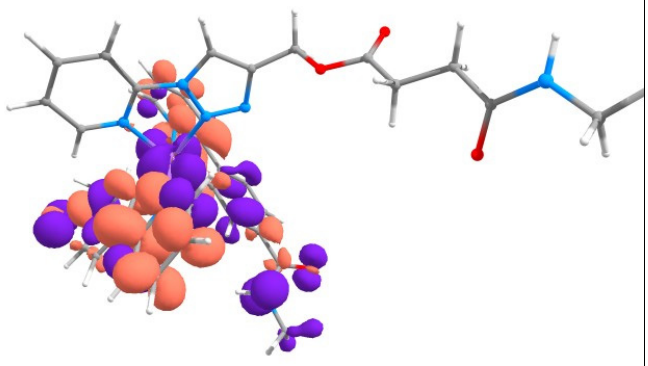

$S_0 \rightarrow S_3$

Donor	Acceptor			
	Ir	N^N2	N^C	N^C’
Ir	0.003	0.010	0.076	0.055
N^N2	0.000	0.002	0.013	0.009
N^C	0.008	0.030	0.226	0.165
N^C’	0.008	0.028	0.212	0.154

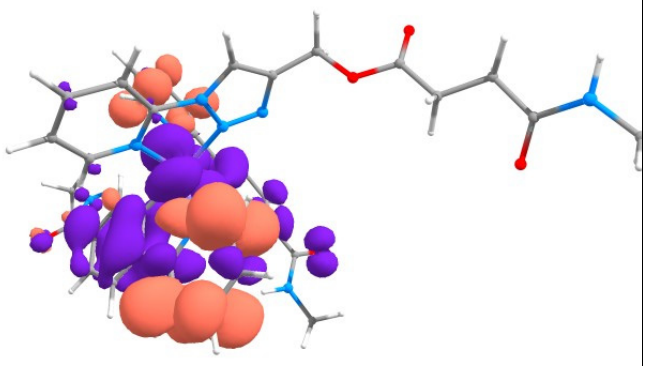

$S_0 \rightarrow S_4$

Donor	Acceptor			
	Ir	N^N2	N^C	N^C’
Ir	0.006	0.005	0.156	0.097
N^N2	0.001	0.001	0.022	0.014
N^C	0.009	0.008	0.244	0.151
N^C’	0.006	0.006	0.170	0.106

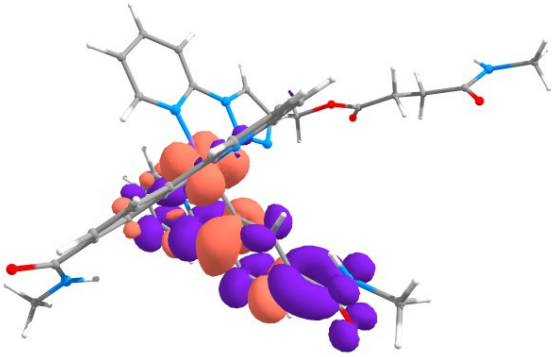

$T_1 \rightarrow S_0$

Donor	Acceptor			
	Ir	N^N2	N^C	N^C’
Ir	0.005	0.000	0.001	0.019
N^N2	0.004	0.000	0.001	0.012
N^C	0.009	0.001	0.002	0.030
N^C’	0.196	0.014	0.033	0.673

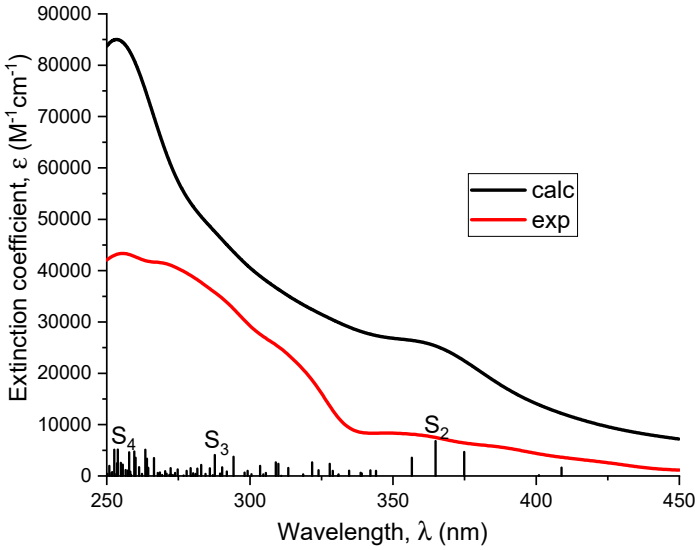

Figure S21. Absorption spectra of **Ir3**: experimental (red) and calculated (black) lines with oscillator strengths of electronic transitions (bars).

Table S7. Calculated absorption maxima (λ) and oscillator strengths (f) of complex **Ir3**.

Transitions	λ_{abs}, nm	*f*	Contribution of main NTO pair in transition (%)
S_0-S_4	254	0.14	44
S_0-S_3	288	0.11	46
S_0-S_2	365	0.18	93
S_0-S_1	453	0.03	95

Table S8.The decrease (violet) and increase (terracotta) of electron density for most intensive electronic absorption transitions of **Ir3**. The data for the corresponding interfragment charge transfer (IFCT) are given below the figures. Diagonal values represent intraligand transitions, off-diagonal values represent a charge transfer from “Donor” to “Acceptor”.

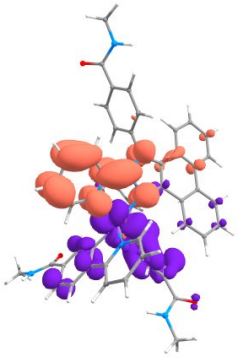

$S_0 \rightarrow S_1$

Donor	Acceptor			
	Ir	N^N3	N^C	N^C’
Ir	0.006	0.337	0.005	0.003
N^N3	0.003	0.153	0.002	0.001
N^C	0.005	0.311	0.005	0.003
N^C’	0.003	0.159	0.003	0.001

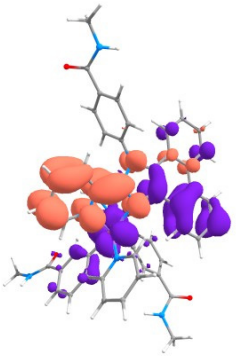

$S_0 \rightarrow S_2$

Donor	Acceptor			
	Ir	N^N3	N^C	N^C’
Ir	0.006	0.338	0.005	0.003
N^N3	0.008	0.470	0.008	0.004
N^C	0.001	0.069	0.001	0.001
N^C’	0.001	0.084	0.001	0.001

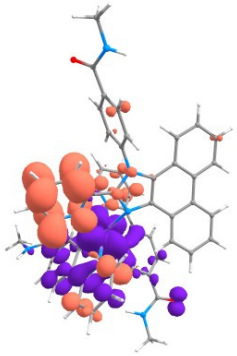

$S_0 \rightarrow S_3$

Donor	Acceptor			
	Ir	N^N3	N^C	N^C’
Ir	0.006	0.167	0.098	0.082
N^N3	0.001	0.036	0.021	0.018
N^C	0.003	0.095	0.055	0.046
N^C’	0.006	0.176	0.103	0.086

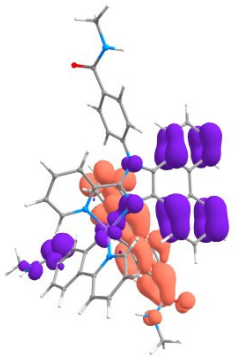

$S_0 \rightarrow S_4$

Donor	Acceptor			
	Ir	N^N3	N^C	N^C’
Ir	0.003	0.025	0.093	0.023
N^N3	0.010	0.084	0.314	0.079
N^C	0.002	0.019	0.073	0.018
N^C’	0.005	0.044	0.164	0.041

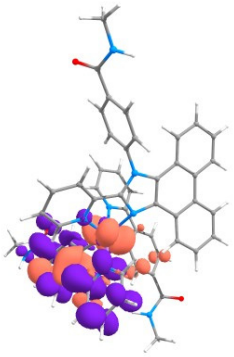

$T_1 \rightarrow S_0$

Donor	Acceptor			
	Ir	N^N3	N^C	N^C’
Ir	0.009	0.001	0.002	0.018
N^N3	0.010	0.001	0.002	0.019
N^C	0.004	0.000	0.001	0.008
N^C’	0.277	0.031	0.070	0.546

Optimized structures data

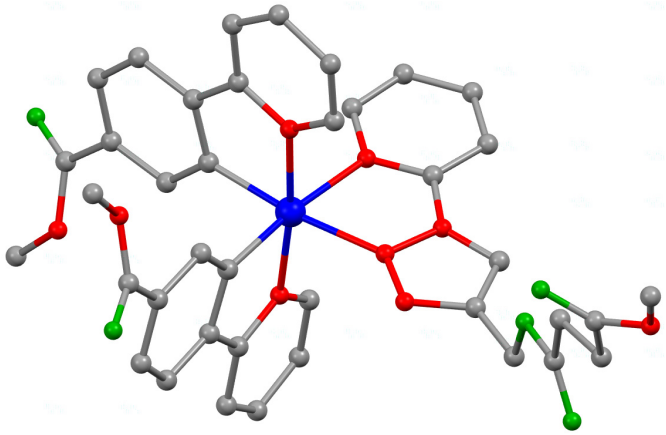

Figure S22. Optimized structure of the model **Ir2-0** complex (hydrogen atoms are omitted for clarity). The calculations have been simplified by substitution of OEG pendants in **Ir2** complex with methyl groups in **Ir2-0** structure. Atom colors: Ir–blue; N–red; O–green; C–gray.

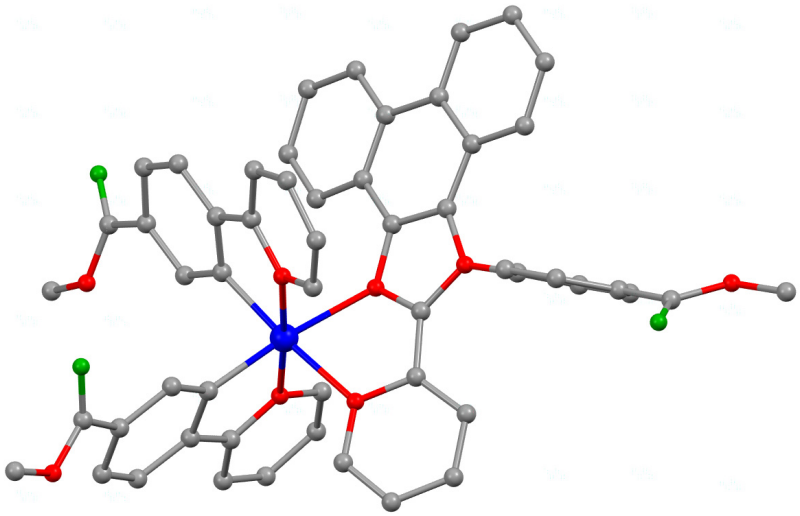

Figure S23. Optimized structure of the model **Ir3-0** complex (hydrogen atoms are omitted for clarity). The calculations have been simplified by substitution of OEG pendants in **Ir3** complex with methyl groups in **Ir3-0** structure. Atom colors: Ir–blue; N–red; O–green; C–gray.

Table S9. The key structural parameters of complex **Ir1-0** (R = Me) and its literature analog [8].

Complex Ir1	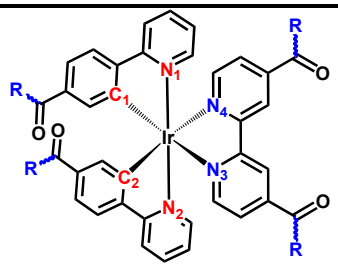	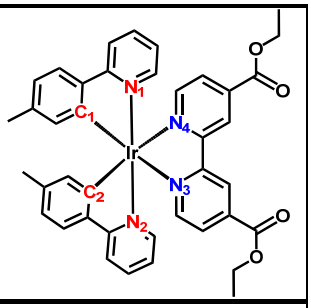
Distances, A°		
Ir-C1	2.003	2.033(12)
Ir-N1	2.065	2.054(10)
Ir-C2	2.003	2.017(13)
Ir-N2	2.065	2.044(11)
Ir-N3	2.137	2.130(10)
Ir-N4	2.138	2.145(9)
Angles, °		
N1-Ir-C1	80.72	80.5(5)
N2-Ir-C2	80.74	81.1(5)
N3-Ir-N4	77.05	76.4(4)
C1-Ir-C2	88.34	88.7(5)
C2-Ir-N1	94.78	94.3(5)
C2-Ir-N4	174.12	176.8(5)
C1-Ir-N2	94.67	94.2(5)
N2-Ir-N4	97.08	99.8(4)
N4-Ir-N1	87.79	85.7(4)
N3-Ir-N2	88.05	88.3(4)
N3-Ir-N1	96.95	97.2(4)
N3-Ir-C1	174.02	170.7(4)
N3-Ir-C2	97.37	100.5(5)
N2-Ir-N1	173.71	173.1(4)
C1-Ir-N4	97.30	94.4(4)

Table S9. The key structural parameters of complex **Ir2-0** (R = Me) and its literature analog [9].

Complex Ir2	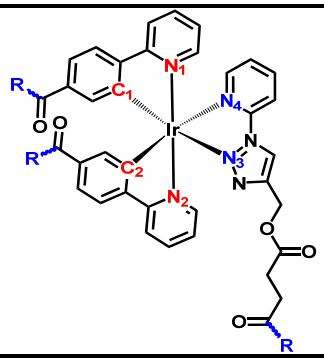	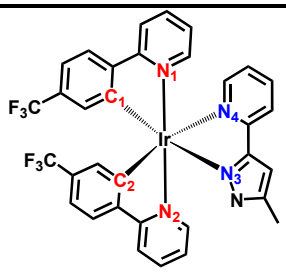
Distances, A°		
Ir-C1	1.997	2.035(13)
Ir-N1	2.066	2.052(12)
Ir-C2	2.001	2.034(13)
Ir-N2	2.067	2.043(10)
Ir-N3	2.119	2.103(9)
Ir-N4	2.161	2.144(11)
Angles, °		
N1-Ir-C1	80.86	79.4(6)
N2-Ir-C2	80.80	79.9(5)
N3-Ir-N4	75.97	75.6(4)
C1-Ir-C2	88.90	92.2(5)
C2-Ir-N1	94.54	95.6(5)
C2-Ir-N4	173.73	171.2(5)
C1-Ir-N2	94.40	96.9(5)
N2-Ir-N4	96.56	93.9(4)
N4-Ir-N1	88.53	90.9(4)
N3-Ir-N2	88.72	92.1(4)
N3-Ir-N1	96.52	92.3(4)
N3-Ir-C1	172.62	167.4(5)
N3-Ir-C2	98.22	98.1(4)
N2-Ir-N1	173.46	174.1(4)
C1-Ir-N4	97.00	94.8(5)

Table S9. The key structural parameters of complex **Ir3-0** (R = Me) and its literature analog [10].

Complex Ir3	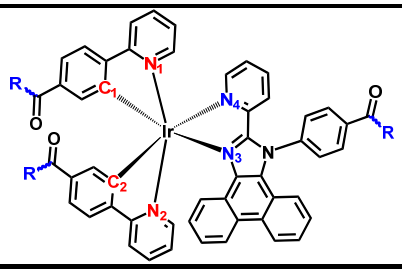	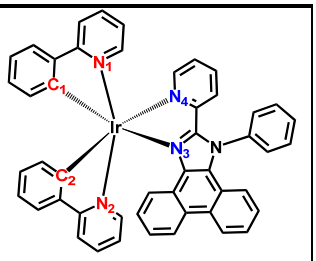
Distances, A°		
Ir-C1	1.990	1.998(3)
Ir-N1	2.052	2.035(3)
Ir-C2	2.002	2.018(3)
Ir-N2	2.069	2.051(3)
Ir-N3	2.204	2.242(3)
Ir-N4	2.153	2.166(3)
Angles, °		
N1-Ir-C1	80.95	80.75(12)
N2-Ir-C2	80.41	80.53(12)
N3-Ir-N4	76.26	75.28(10)
C1-Ir-C2	87.22	84.52(13)
C2-Ir-N1	95.50	93.45(12)
C2-Ir-N4	174.94	176.19(1)
C1-Ir-N2	97.54	95.47(12)
N2-Ir-N4	95.47	97.36(10)
N4-Ir-N1	88.68	88.47(10)
N3-Ir-N2	81.80	88.32(10)
N3-Ir-N1	100.23	96.54(10)
N3-Ir-C1	172.37	167.65(10)
N3-Ir-C2	100.12	107.71(11)
N2-Ir-N1	175.73	173.23(10)
C1-Ir-N4	96.28	92.55(11)

References

1. Frisch, M.J.; Trucks, G.W.; Schlegel, H.B.; Scuseria, G.E.; Robb, M.A.; Cheeseman, J.R.; Scalmani, G.; Barone, V.; Petersson, G.A.; Nakatsuji, H.; Li, X.; et al. Gaussian 16, Revision B.01, 2016.

2. Austin, A.; Petersson, G.A.; Frisch, M.J.; Dobek, F.J.; Scalmani, G.; Throssell, K. A Density Functional with Spherical Atom Dispersion Terms. *J. Chem. Theory Comput.* **2012**, *8*, 4989–5007, doi:10.1021/ct300778e.

3. Dolg, M.; Wedig, U.; Stoll, H.; Preuss, H. Energy-adjusted ab initio pseudopotentials for the first row transition elements. *J. Chem. Phys.* **1987**, *86*, 866–872, doi:10.1063/1.452288.

4. Tomasi, J.; Mennucci, B.; Cammi, R. Quantum Mechanical Continuum Solvation Models. *Chem. Rev.* **2005**, *105*, 2999–3094, doi:10.1021/cr9904009.

5. O'boyle, N.M.; Tenderholt, A.L.; Langner, K.M. cclib: A library for package-independent computational chemistry algorithms. *J. Comput. Chem.* **2008**, *29*, 839–845, doi:https://doi.org/10.1002/jcc.20823.

6. Martin, R.L. Natural transition orbitals. *J. Chem. Phys.* **2003**, *118*, 4775–4777, doi:10.1063/1.1558471.

7. Lu, T.; Chen, F. Multiwfn: A multifunctional wavefunction analyzer. *J. Comput. Chem.* **2012**, *33*, 580–592, doi:10.1002/jcc.22885.

8. Hanss, D.; Freys, J.C.; Bernardinelli, G.; Wenger, O.S. Cyclometalated Iridium(III) Complexes as Photosensitizers for Long-Range Electron Transfer: Occurrence of a Coulomb Barrier. *Eur. J. Inorg. Chem.* **2009**, *2009*, 4850–4859, doi:https://doi.org/10.1002/ejic.200900673.

9. Su, N.; Lu, G.-Z.; Zheng, Y.-X. Highly efficient green electroluminescence of iridium(iii) complexes based on (1H-pyrazol-5-yl)pyridine derivatives ancillary ligands with low efficiency roll-off. *J. Mater. Chem. C* **2018**, *6*, 5778–5784, doi:10.1039/C8TC01182F.

10. Solomatina, A.I.; Kuznetsov, K.M.; Gurzhiy, V. V; Pavlovskiy, V. V; Porsev, V. V; Evarestov, R.A.; Tunik, S.P. Luminescent organic dyes containing a phenanthro[9,10-D]imidazole core and [Ir(N^C)(N^N)]+ complexes based on the cyclometalating and diimine ligands of this type. *Dalt. Trans.* **2020**, *49*, 6751–6763, doi:10.1039/D0DT00568A.